

An Application of Wiener Hermite Expansion to Non-linear Evolution of Dark Matter

N. S. Sugiyama

Astronomical Institute, Graduate School of Science, Tohoku University, Sendai 980-8578, Japan

T. Futamase

Astronomical Institute, Graduate School of Science, Tohoku University, Sendai 980-8578, Japan

sugiyama@astr.tohoku.ac.jp

ABSTRACT

We apply the Wiener Hermite (WH) expansion to the non-linear evolution of Large-Scale Structure, and obtain an approximate expression for the matter power spectrum in full order of the expansion. This method allows us to expand any random function in terms of an orthonormal bases in space of random functions in such a way that the first order of the expansion expresses the Gaussian distribution, and others are the deviation from the Gaussianity. It is proved that the Wiener Hermite expansion is mathematically equivalent with the Γ -expansion approach in the Renormalized Perturbation Theory (RPT). While an exponential behavior in the high- k limit has been proved for the mass density and velocity fluctuations of Dark Matter in the RPT, we reprove the behavior in the context of the Wiener Hermite expansion using the result of Standard Perturbation Theory (SPT). We propose a new approximate expression for the matter power spectrum which interpolates the low- k expression corresponding to 1-loop level in SPT and the high- k expression obtained by taking a high- k limit of the WH expansion. The validity of our prescription is specifically verified by comparing with the 2-loop solutions of the SPT. The proposed power spectrum agrees with the result of N -body simulation with the accuracy better than 1% or 2% in a range of the BAO scales, where the wave number is about $k = 0.2 \sim 0.4 h\text{Mpc}^{-1}$ at $z = 0.5\text{-}3.0$. This accuracy is comparable to or slightly less than the ones in the Closure Theory whose the fractional difference from N body result is within 1%. A merit of our method is that the computational time is very short because only single and double integrals are involved in our solution.

1. Introduction

Precise measurements of matter power spectrum in the large-scale structure is a powerful tool not only to investigate the details of the structure formation, but also to estimate the cosmological parameters. For example, the precise measurements of the Baryon Acoustic Oscillation

(BAO) in the matter power spectrum observed by SDSS survey has been emerged as a powerful tool to estimate cosmological parameters (Eisenstein, Hu, & Tegmark 1998; Matsubara 2004; Eisenstein et al. 2005; Seo & Eisenstein 2003; Blake & Glazebrook 2003; Glazebrook & Blake 2005; Shoji, Jeong, & Komatsu 2009; Padmanabhan & White 2008). Also the observation of cosmic shear in near future is expected to give a useful constraint on the nature of dark energy. Obviously the proper understanding of the observed power spectrum becomes possible only if an accurate theoretical prediction is available which requires a good understanding of the non-linear evolution of dark matter perturbation, the relation between dark matter and baryonic matter (bias effect) and redshift distortion effect. There have been various studies and progresses on the theoretical calculations of the power spectrum, but it is still useful and required to have more accurate theoretical treatment. In this paper, we give a new approach to describe the non-linear evolution of Dark Matter. It is called “Wiener Hermite expansion method”, where the stochastic nature of the cosmological density perturbation is manifestly used and the stochastic variables are expanded in terms of an orthonormal basis in the space of stochastic functions. The method is developed in 1970s for the application to turbulent theory in fluid dynamics and applied to cosmological turbulent theory by one of the present authors. The method gives us a coupled equation at each perturbative order, even at the first order in such a way the lower order quantities is modified by higher order quantities. This it is totally different from the usual perturbation theory where lower order quantities are never influenced by higher order quantities. Thus it gives us a prescription of renormalization of higher order effects and the precise meaning is described below. It has a nice feature that each expansion coefficient has a clear statistical meaning, namely the coefficient of the first, second and third terms in the expansion express the amplitude of Gaussianity, the skewness and kurtosis, respectively. Thus each term corresponds directly to an appropriate n-point correlation function.

We mention here some details on the previous approaches in connection with ours. It has been known for some time that the standard perturbation theory of cosmological perturbation (which we call SPT) can be analytically solved in Einstein-de Sitter universe in integral forms (Fry 1984; Goroff et al. 1986; Suto & Sasaki 1991; Makino, Sasaki, & Suto 1992; Jain & Bertschinger 1994; Scoccimarro & Frieman 1996; Bernardeau et al. 2002). When it is considered up to the third order in SPT (1-loop level), the analytical predictions describe the non-linearity well at sufficiently high redshifts (Jeong & Komatsu 2006, 2009). However, the predictions are insufficient yet at the observable low redshifts ($z = 0-3$), and we need to consider further non-linear effects. Furthermore, it is computationally expensive to deal with the higher order corrections in the SPT. Therefore, various modification of SPT have been proposed in the past. One of the main approach is the “Renormalized Perturbation Theory” (RPT) (Crocce & Scoccimarro 2006a,b, 2008), where the basic equations for fluid describing the matter perturbation are rewritten in a convenient compact form in order to use a diagramatic technique developed in quantum field theory (Scoccimarro 1998). Further modification have been considered, e.g., the “Closure Theory” (Taruya et al. 2009; Hiramatsu & Taruya 2009), the “Time Renormalization Group” (TRG) approach (Pietroni 2008), and the “ Γ -expansion approach” using Multi-Point Propagators

(Bernardeau, Crocce, & Scoccimarro 2008; Bernardeau, Crocce, & Sefusatti 2010; Bernardeau, Van de Rijt, & Vernizzi 2012; Bernardeau, Crocce, & Scoccimarro 2012). Other many new methods have been also studied (McDonald 2007; Valageas 2004; Matarrese & Pietroni 2007). On the other hand, there are also an approach to the large-scale structure in the framework of the Lagrangian picture, called “Lagrangian Resummation Theory” (LRT) (Matsubara 2008b, 2011, 2008a; Okamura, Taruya, & Matsubara 2011).

It will be shown that our approach is mathematically equivalent to the Γ -expansion approach, but it still has nice features described above and gives us a very convenient expression for the matter power spectrum described below. In almost all modified perturbation theories, the resummation of the non-linear effects, which means the partial summation of the infinite order in the SPT, is considered. This implies that any modified perturbative expansion methods should be described in the context of the SPT. In this paper, we use only the SPT, and reprove various properties about cosmological perturbations, e.g., their behavior in the small scale limit (high- k limit) proved in the context in the RPT (Crocce & Scoccimarro 2006a,b; Bernardeau, Van de Rijt, & Vernizzi 2012).

Since the low- k solutions can be safely computed using the SPT, it have been attempted to derive the more precise solutions of cosmological perturbations by interpolating between the 1-loop results and the high- k behavior (Crocce & Scoccimarro 2006b; Bernardeau, Crocce, & Scoccimarro 2012). However, there have been remained somewhat arbitrariness for these prescription. To resolve this problem, we propose a unique interpolation between the low- k solutions and the high- k ones by assuming that the higher order solutions in perturbation theory are well approximated by the ones in the high- k limit. Then, we compute only up to 1-loop level corrections in SPT precisely, and replace the higher order corrections into the ones calculated in the high- k limit. In this way we obtain an approximate full power spectrum, and the power spectrum shows a very good agreement with N -body results up to rather high- k (about $\lesssim 0.2\text{-}0.4 h\text{Mpc}^{-1}$) within 1 or 2 % accuracy.

This paper is organized as follows. In Section 2, we first explain the stochastic properties which should be satisfied by the density and velocity perturbations of Dark Matter. In Section 3, we briefly review the Standard Perturbation Theory which will be used later. Then the Wiener Hermite expansion technique is explained in our context in Section 4. The relationship to the SPT and the WH expansion method is established there, and this also shows the mathematical equivalence between WH expansion and Γ -expansion. In Section 5, we reprove the high- k limit behavior of the cosmological perturbations in the context of the SPT, and propose an approximate full power spectrum where the lower order corrections is calculated only up to 1-loop levels in SPT and the higher order corrections is replaced into the high- k solutions. In Section 6, we compare our result with some other analytic predictions and N -body simulations. We compute the two-point correlation function in Section 7. We summarize our work and discuss future works in Section 8.

2. Stochastic Nature of Cosmological Perturbations

After de-coupling, baryon and Dark Matter fluctuations are tightly coupled by the gravitational force, and the evolution can be then described by the pressureless fluid equations (continuity equation and Euler equation) with the Poisson equation for the Newton gravity. Thus our basic equations are as follows (Bernardeau et al. 2002):

$$\begin{aligned}\frac{\partial \rho}{\partial t} + \nabla \cdot [\rho \mathbf{v}] &= 0, \\ \frac{\partial \mathbf{v}}{\partial t} + \mathbf{v} \cdot \nabla \mathbf{v} &= -\nabla \phi, \\ \nabla^2 \phi + \Lambda c^2 &= 4\pi G \rho,\end{aligned}\tag{1}$$

where ρ , \mathbf{v} , and ϕ denote the mass density, velocity and gravitational potential, respectively, and Λ is cosmological constant.

When we transform the spatial coordinates as $\mathbf{x} \rightarrow a\mathbf{x}$ and redefine the velocity as $\mathbf{v} \equiv \dot{a}\mathbf{x} + \mathbf{u}$, where a is the scale factor and \mathbf{u} is the peculiar velocity, we can express Eq. (1) as

$$\frac{\partial \rho(\tau, \mathbf{x})}{\partial \tau} + 3\mathcal{H}(\tau)\rho(\tau, \mathbf{x}) + \nabla \cdot [\rho(\tau, \mathbf{x})\mathbf{u}(\tau, \mathbf{x})] = 0,\tag{2}$$

$$\frac{\partial \mathbf{u}(\tau, \mathbf{x})}{\partial \tau} + \mathcal{H}(\tau)\mathbf{u}(\tau, \mathbf{x}) + [\mathbf{u} \cdot \nabla] \mathbf{u}(\tau, \mathbf{x}) = -\nabla \Phi(\tau, \mathbf{x}),\tag{3}$$

$$\frac{\nabla^2 \phi}{a^2} + \Lambda c^2 = 4\pi G \rho,\tag{4}$$

where the conformal time τ is defined as $ad\tau \equiv dt$, and the conformal Hubble parameter \mathcal{H} is define as $\mathcal{H} = aH$, where H is the Hubble parameter. We further defined the cosmological gravitational potential as $\Phi \equiv \phi + \frac{1}{2}\mathcal{H}'x^2$.

In the standard cosmological perturbation theory, any physical quantities are decomposed into the background part and the perturbative part. The background part of the mass density $\bar{\rho}$ is defined as

$$\bar{\rho}(t) \equiv \langle \rho(\mathbf{x}, t) \rangle = \langle \rho(0, t) \rangle.\tag{5}$$

where $\langle \dots \rangle$ denotes the ensemble average and we used the translation symmetry of the ensemble average. On the other hand, the peculiar velocity \mathbf{u} has no background part because of the rotation symmetry in the averaged sense. Therefore, the perturbative part of the mass density and the peculiar velocity has the property that their ensemble average are zero by definition:

$$\langle \delta\rho \rangle = \langle \mathbf{u} \rangle = 0.\tag{6}$$

Averaging the above set of equations, we obtain the following background equations.

$$\frac{\partial \bar{\rho}}{\partial \tau} + 3\mathcal{H}\bar{\rho} = 0,\tag{7}$$

$$\frac{\partial \mathcal{H}}{\partial \tau} = -\frac{4\pi G}{3}\bar{\rho}a^2 + \frac{1}{3}\Lambda c^2 a^2, \quad (8)$$

By integrating Eq. (8), we find the usual Friedman equation,

$$\mathcal{H}^2 + c^2 \mathcal{K} = \frac{8\pi G}{3}a^2 \bar{\rho} + \frac{1}{3}\Lambda c^2 a^2, \quad (9)$$

where the integral constant \mathcal{K} is interpreted as the spatial curvature.

By subtracting the background equations from Eq. (2) (3), we find the our basic equations in Fourier space as follows,

$$\delta'(\tau, \mathbf{k}) + \theta(\tau, \mathbf{k}) = - \int \frac{dk_1^3}{(2\pi)^3} \int \frac{dk_2^3}{(2\pi)^3} (2\pi)^3 \delta_D(\mathbf{k}_1 + \mathbf{k}_2 - \mathbf{k}) \alpha(\mathbf{k}_1, \mathbf{k}_2) \theta(\tau, \mathbf{k}_1) \delta(\tau, \mathbf{k}_2), \quad (10)$$

$$\theta'(\tau, \mathbf{k}) + \mathcal{H}\theta(\tau, \mathbf{k}) + \frac{3}{2}\Omega_m \mathcal{H}^2 \delta(\tau, \mathbf{k}) = - \int \frac{dk_1^3}{(2\pi)^3} \int \frac{dk_2^3}{(2\pi)^3} (2\pi)^3 \delta_D(\mathbf{k}_1 + \mathbf{k}_2 - \mathbf{k}) \beta(\mathbf{k}_1, \mathbf{k}_2) \theta(\tau, \mathbf{k}_1) \theta(\tau, \mathbf{k}_2), \quad (11)$$

where $\delta \equiv \delta\rho/\bar{\rho}$ and $\theta \equiv \partial_i \mathbf{u}^i$ denotes the divergence of velocity, and δ_D denotes the three-dimensional Dirac delta distribution. We neglected the vorticity $\mathbf{w} \equiv \nabla \times \mathbf{u}$ because the vorticity have been zero if its initial value is zero, and even if its initial value is non-zero, it decays due to the expansion of the universe. The functions

$$\alpha(\mathbf{k}_1, \mathbf{k}_2) \equiv \frac{(\mathbf{k}_1 + \mathbf{k}_2) \cdot \mathbf{k}_1}{k_1^2}, \quad (12)$$

$$\beta(\mathbf{k}_1, \mathbf{k}_2) \equiv \frac{|\mathbf{k}_1 + \mathbf{k}_2|^2 (\mathbf{k}_1 \cdot \mathbf{k}_2)}{2k_1^2 k_2^2}, \quad (13)$$

encode the non-linearity of the evolution, and satisfy the conditions

$$\alpha(\mathbf{k}, -\mathbf{k}) = \beta(\mathbf{k}, -\mathbf{k}) = 0, \quad (14)$$

Note that this decomposition between background and perturbation is exact in Newtonian gravity, namely there are no backreaction terms generated from the ensemble average in Newton gravity, and the perturbative parts δ and θ obeying Eq. (10) (11) naturally satisfy the stochastic condition in Eq. (6): $\langle \delta \rangle = \langle \theta \rangle = 0$. More specifically, when the solutions for non-linear equations are expanded perturbatively, the property that their ensemble averages are zero is not guaranteed in general, and thus redefinition of the perturbation variables such as $\delta \rightarrow \delta - \langle \delta \rangle$ is necessary. In the case of cosmological SPT, the average such as $\langle \delta(\mathbf{k}) \rangle$ is proportional to $\delta_D(\mathbf{k})$, which is interpreted as the vacuum bubble diagrams in the diagrammatical picture and contributes only in infinite large scales. This means we really needs a redefinition of cosmological background. However, we do not need to consider this prescriptions for perturbative variables in Eq. (10) (11). This is a special feature on Newtonian gravity. It will be interesting to see how the backreaction look like in the case of general relativistic gravity in our approach.

3. Review of Standard Perturbation Theory

We here explain very briefly SPT which will be used later. It is well known that the solutions in the case of Einstein-de Sitter universe, where $\Omega_m = 1$ and $\Omega_\Lambda = 0$, can be described by integral forms analytically in SPT. More explicitly, the solution may be written in the following perturbative form,

$$\delta(z, \mathbf{k}) = \sum_{n=1}^{\infty} a^n \delta_n(\mathbf{k}), \quad \theta(z, \mathbf{k}) = -\mathcal{H} \sum_{n=1}^{\infty} a^n \theta_n(\mathbf{k}), \quad (15)$$

where the scale factor a is a growing mode solution in the linearized theory. When the scale factor a is small, the series are dominated by their first term, that is, by linearized theory. The relation between the time-independent coefficients $\delta_1(\mathbf{k})$ and $\theta_1(\mathbf{k})$ is shown from the continuity equation Eq. (10) as $\delta_1(\mathbf{k}) = \theta_1(\mathbf{k}) \equiv \delta_L(\mathbf{k})$, and the time-independent linear power spectrum for $\delta_L(\mathbf{k})$ is defined as

$$\langle \delta_L(\mathbf{k}) \delta_L(\mathbf{k}') \rangle = (2\pi)^3 \delta_D(\mathbf{k} + \mathbf{k}') P_L(k), \quad (16)$$

where the amplitude of wave vector is expressed as $k \equiv |\mathbf{k}|$.

Then, the coefficients $\delta_n(\mathbf{k})$ and $\theta_n(\mathbf{k})$ is described as follows,

$$\delta_n(\mathbf{k}) = \int \frac{d^3 q_1}{(2\pi)^3} \cdots \frac{d^3 q_n}{(2\pi)^3} (2\pi)^3 \delta_D(\mathbf{k} - \mathbf{q}_{1n}) F_n(\mathbf{q}_1, \dots, \mathbf{q}_n) \delta_L(\mathbf{q}_1) \cdots \delta_L(\mathbf{q}_n), \quad (17)$$

$$\theta_n(\mathbf{k}) = \int \frac{d^3 q_1}{(2\pi)^3} \cdots \frac{d^3 q_n}{(2\pi)^3} (2\pi)^3 \delta_D(\mathbf{k} - \mathbf{q}_{1n}) G_n(\mathbf{q}_1, \dots, \mathbf{q}_n) \delta_L(\mathbf{q}_1) \cdots \delta_L(\mathbf{q}_n), \quad (18)$$

where $\mathbf{q}_{1n} \equiv \mathbf{q}_1 + \mathbf{q}_2 + \cdots + \mathbf{q}_n$ and F_n and G_n is completely-symmetrized functions for the wave vectors $\{\mathbf{q}_1, \mathbf{q}_2, \dots, \mathbf{q}_n\}$. The functions F_n and G_n are constructed according to the following recursion relations ($n \geq 1$) (Goroff et al. 1986; Bernardeau et al. 2002):

$$F_{n+1}(\mathbf{q}_1, \dots, \mathbf{q}_{n+1}) = \sum_{m=1}^n \frac{G_m(\mathbf{q}_1, \dots, \mathbf{q}_m)}{(2n+5)n} \left[(2n+3)\alpha(\mathbf{k}_1, \mathbf{k}_2) F_{n+1-m}(\mathbf{q}_{m+1}, \dots, \mathbf{q}_{n+1}) \right. \\ \left. + 2\beta(\mathbf{k}_1, \mathbf{k}_2) G_{n+1-m}(\mathbf{q}_{m+1}, \dots, \mathbf{q}_{n+1}) \right], \quad (19)$$

$$G_{n+1}(\mathbf{q}_1, \dots, \mathbf{q}_{n+1}) = \sum_{m=1}^n \frac{G_m(\mathbf{q}_1, \dots, \mathbf{q}_m)}{(2n+5)n} \left[3\alpha(\mathbf{k}_1, \mathbf{k}_2) F_{n+1-m}(\mathbf{q}_{m+1}, \dots, \mathbf{q}_{n+1}) \right. \\ \left. + (2n+2)\beta(\mathbf{k}_1, \mathbf{k}_2) G_{n+1-m}(\mathbf{q}_{m+1}, \dots, \mathbf{q}_{n+1}) \right], \quad (20)$$

where $\mathbf{k}_1 \equiv \mathbf{q}_1 + \cdots + \mathbf{q}_m$, $\mathbf{k}_2 \equiv \mathbf{q}_{m+1} + \cdots + \mathbf{q}_{n+1}$ and $F_1 = G_1 = 1$.

For $n = 1$, we have

$$F_2(\mathbf{k}_1, \mathbf{k}_2) = \frac{5}{7} + \frac{1}{2} \frac{\mathbf{k}_1 \cdot \mathbf{k}_2}{k_1 k_2} \left(\frac{k_1}{k_2} + \frac{k_2}{k_1} \right) + \frac{2}{7} \frac{(\mathbf{k}_1 \cdot \mathbf{k}_2)^2}{k_1^2 k_2^2}, \quad (21)$$

$$G_2(\mathbf{k}_1, \mathbf{k}_2) = \frac{3}{7} + \frac{1}{2} \frac{\mathbf{k}_1 \cdot \mathbf{k}_2}{k_1 k_2} \left(\frac{k_1}{k_2} + \frac{k_2}{k_1} \right) + \frac{4}{7} \frac{(\mathbf{k}_1 \cdot \mathbf{k}_2)^2}{k_1^2 k_2^2}. \quad (22)$$

The stochastic property $\langle \delta \rangle = \langle \theta \rangle = 0$ is specifically shown from these solutions. When we consider the average of Eq. (17), we only have to consider the each coefficient δ_n and θ_n due to the linearity of the ensemble average. The ensemble average for δ_n is

$$\begin{aligned} \langle \delta_n(\mathbf{k}) \rangle &= \int \frac{d^3 q_1}{(2\pi)^3} \dots \frac{d^3 q_n}{(2\pi)^3} (2\pi)^3 \delta_D(\mathbf{k} - \mathbf{q}_{1n}) F_n(\mathbf{q}_1, \dots, \mathbf{q}_n) \langle \delta_L(\mathbf{q}_1) \dots \delta_L(\mathbf{q}_n) \rangle \\ &= \int \frac{d^3 q_1}{(2\pi)^3} \dots \frac{d^3 q_n}{(2\pi)^3} (2\pi)^3 \delta_D(\mathbf{k} - \mathbf{q}_{1n}) F_n(\mathbf{q}_1, \dots, \mathbf{q}_n) (2\pi)^2 \delta_D(\mathbf{q}_{1n}) B(\mathbf{q}_1, \dots, \mathbf{q}_n), \end{aligned} \quad (23)$$

where $B(\mathbf{q}_1, \dots, \mathbf{q}_n)$ is defined as

$$\langle \delta_L(\mathbf{q}_1) \dots \delta_L(\mathbf{q}_n) \rangle \equiv (2\pi)^3 \delta_D(\mathbf{q}_{1n}) B(\mathbf{q}_1, \dots, \mathbf{q}_n). \quad (24)$$

When the function F_n in Eq. (19) substitute into Eq. (23), $\mathbf{k}_1 + \mathbf{k}_2 = \mathbf{q}_{1n} = 0$ is satisfied due to the Dirac delta function in Eq. (23), and the functions $\alpha(\mathbf{k}_1, \mathbf{k}_2)$ and $\beta(\mathbf{k}_1, \mathbf{k}_2)$ become zero from Eq. (14). Then, it is shown that the function F_n in Eq. (23) becomes zero, and $\langle \delta \rangle = 0$. The similar discussion can be applied for θ .

Note that this stochastic property is independent to the initial conditions of δ_L , that is, the initial condition can have the primordial Non-Gaussianity.

4. Wiener Hermite Expansion

Now, we explain our expansion method for δ and θ . Our expansion scheme should satisfy the following two properties. First it is known observationally and theoretically that the cosmological perturbations in the universe has nearly Gaussian distribution. Thus the first order in our expansion should express the Gaussian distribution. Second, the expansion scheme should respect the stochastic condition of the cosmological perturbations, $\langle \delta \rangle = \langle \theta \rangle = 0$. According to these two conditions, we adopt the Wiener Hermite expansion as our expansion method.

4.1. Definition of the Wiener Hermite expansion

In the Wiener Hermite expansion, the perturbation variables δ and θ are expanded as follows,

$$\delta(z, \mathbf{k}) = \sum_{r=1}^{\infty} \int \frac{d^3 p_1}{(2\pi)^3} \dots \int \frac{d^3 p_r}{(2\pi)^3} (2\pi)^3 \delta_D(\mathbf{k} - \mathbf{p}_{1r}) \delta_{\text{WH}}^{(r)}(z, \mathbf{p}_1, \dots, \mathbf{p}_r) H^{(r)}(\mathbf{p}_1, \dots, \mathbf{p}_r), \quad (25)$$

$$\theta(z, \mathbf{k}) = \sum_{r=1}^{\infty} \int \frac{d^3 p_1}{(2\pi)^3} \cdots \int \frac{d^3 p_r}{(2\pi)^3} (2\pi)^3 \delta_D(\mathbf{k} - \mathbf{p}_{1r}) \theta_{\text{WH}}^{(r)}(z, \mathbf{p}_1, \dots, \mathbf{p}_r) H^{(r)}(\mathbf{p}_1, \dots, \mathbf{p}_r), \quad (26)$$

where the functions $H^{(r)}$ $\{r = 1, 2, \dots\}$ are the stochastic variables. The first order $H^{(1)}$ is a white noise function which satisfies the Gaussian distribution,

$$\langle H^{(1)}(\mathbf{k}_1) H^{(1)}(\mathbf{k}_2) \rangle = (2\pi)^3 \delta_D(\mathbf{k}_1 + \mathbf{k}_2), \quad (27)$$

and we further define higher order bases $H^{(r)}$ $\{r = 2, 3, 4, \dots\}$ in the expansion as follows.

$$\begin{aligned} H^{(2)}(\mathbf{k}_1, \mathbf{k}_2) &\equiv H^{(1)}(\mathbf{k}_1) H^{(1)}(\mathbf{k}_2) - (2\pi)^3 \delta_D(\mathbf{k}_1 + \mathbf{k}_2), \\ H^{(3)}(\mathbf{k}_1, \mathbf{k}_2, \mathbf{k}_3) &\equiv H^{(1)}(\mathbf{k}_1) H^{(1)}(\mathbf{k}_2) H^{(1)}(\mathbf{k}_3) - H^{(1)}(\mathbf{k}_1) (2\pi)^3 \delta_D(\mathbf{k}_2 + \mathbf{k}_3), \\ &\quad - H^{(1)}(\mathbf{k}_2) (2\pi)^3 \delta_D(\mathbf{k}_1 + \mathbf{k}_3) - H^{(1)}(\mathbf{k}_3) (2\pi)^3 \delta_D(\mathbf{k}_1 + \mathbf{k}_2), \\ H^{(4)}(\mathbf{k}_1, \mathbf{k}_2, \mathbf{k}_3, \mathbf{k}_4) &\equiv \dots, \end{aligned} \quad (28)$$

Thus they becomes an orthonormal bases in the space of stochastic functions, where the ensemble average of $H^{(r)}$ is clearly zero.

$$\langle H^{(r)}(\mathbf{k}_1 \dots \mathbf{k}_r) \rangle = 0, \quad \{r = 1, 2, 3, \dots\}. \quad (29)$$

$$\langle H^{(r)}(\mathbf{k}_1 \dots \mathbf{k}_r) H^{(s)}(\mathbf{k}'_1 \dots \mathbf{k}'_s) \rangle = 0, \quad \{r \neq s\}. \quad (30)$$

Therefore, the stochastic property in Eq. (6) is satisfied by the definition of the Wiener Hermite expansion.

The coefficients of the Wiener Hermite expansion are derived by averaging δ and θ after multiplying the stochastic variable $H^{(r)}$:

$$\begin{aligned} \langle \delta(\mathbf{k}) H^{(r)}(-\mathbf{k}_1, \dots, -\mathbf{k}_r) \rangle &= (2\pi)^3 \delta_D(\mathbf{k} - \mathbf{k}_{1r}) r! \delta_{\text{WH}}^{(r)}(z, \mathbf{k}_1, \dots, \mathbf{k}_r), \\ \langle \theta(\mathbf{k}) H^{(r)}(-\mathbf{k}_1, \dots, -\mathbf{k}_r) \rangle &= (2\pi)^3 \delta_D(\mathbf{k} - \mathbf{k}_{1r}) r! \theta_{\text{WH}}^{(r)}(z, \mathbf{k}_1, \dots, \mathbf{k}_r). \end{aligned} \quad (31)$$

The power spectrum is described in the Wiener Hermite expansion by

$$\begin{aligned} P(z, k) &= \sum_{r=0}^{\infty} (r+1)! \int \frac{d^3 p_1}{(2\pi)^3} \cdots \int \frac{d^3 p_r}{(2\pi)^3} [\delta_{\text{WH}}^{(r+1)}(z, \mathbf{k} - \mathbf{p}_{1r}, \mathbf{p}_1, \dots, \mathbf{p}_r)]^2 \\ &= \sum_{r=0}^{\infty} P_{\text{WH}}^{(r+1)}(z, k), \end{aligned} \quad (32)$$

where the contribution of the $(r+1)$ -th order in the Wiener Hermite expansion to the power spectrum $P_{\text{WH}}^{(r+1)}$ is defined as

$$P_{\text{WH}}^{(r+1)}(z, k) \equiv (r+1)! \int \frac{d^3 p_1}{(2\pi)^3} \cdots \int \frac{d^3 p_r}{(2\pi)^3} [\delta_{\text{WH}}^{(r+1)}(z, \mathbf{k} - \mathbf{p}_{1r}, \mathbf{p}_1, \dots, \mathbf{p}_r)]^2. \quad (33)$$

4.2. Relation between Standard PT and Wiener Hermite Expansion

Since the solutions for any order of the SPT are given in Einstein-de Sitter universe analytically, any new expansion for δ and θ must be described in the context of the SPT. For the linear order, we assume

$$\delta_L(\mathbf{k}) = \delta_1^{(1)}(k)H^{(1)}(\mathbf{k}), \quad P_L(k) = [\delta_1^{(1)}(k)]^2, \quad (34)$$

where the superscript and script indices for $\delta_1^{(1)}$ denote the order of the Wiener Hermite expansion and the SPT, respectively. It is straightforward to include the intrinsic non-Gaussianities as higher order contributions in the WH expansion. From now on, we express as $\delta_1^{(1)}(k) \rightarrow \delta_L(k)$. When we substitute the solutions in the SPT Eqs. (15) (17) and (18) into Eq. (31), we can find the general relation of the solutions between in the SPT and in the Wiener Hermite expansion as follows,

$$\begin{aligned} \delta_{\text{WH}}^{(r+1)}(z, \mathbf{k}_1, \dots, \mathbf{k}_{r+1}) &= \sum_{n=0}^{\infty} a^{2n+r+1} \delta_{2n+r+1}^{(r+1)}(\mathbf{k}_1, \dots, \mathbf{k}_{r+1}), \\ \theta_{\text{WH}}^{(r+1)}(z, \mathbf{k}_1, \dots, \mathbf{k}_{r+1}) &= -\mathcal{H} \sum_{n=0}^{\infty} a^{2n+r+1} \theta_{2n+r+1}^{(r+1)}(\mathbf{k}_1, \dots, \mathbf{k}_{r+1}), \end{aligned} \quad (35)$$

where

$$\begin{aligned} \delta_{2n+r+1}^{(r+1)}(\mathbf{k}_1, \dots, \mathbf{k}_{r+1}) &\equiv \frac{1}{(r+1)!} \frac{(2n+r+1)!}{(2n+1)!} (2n+1)!! \delta_L(k_1) \dots \delta_L(k_{r+1}) \\ &\quad \times \int \frac{d^3 p_1}{(2\pi)^3} \dots \frac{d^3 p_n}{(2\pi)^3} F_{2n+r+1}(\mathbf{k}_1, \dots, \mathbf{k}_{r+1}, \mathbf{p}_1, -\mathbf{p}_1, \dots, \mathbf{p}_n, -\mathbf{p}_n) P_L(p_1) \dots P_L(p_n), \\ \theta_{2n+r+1}^{(r+1)}(\mathbf{k}_1, \dots, \mathbf{k}_{r+1}) &\equiv \frac{1}{(r+1)!} \frac{(2n+r+1)!}{(2n+1)!} (2n+1)!! \delta_L(k_1) \dots \delta_L(k_{r+1}) \\ &\quad \times \int \frac{d^3 p_1}{(2\pi)^3} \dots \frac{d^3 p_n}{(2\pi)^3} G_{2n+r+1}(\mathbf{k}_1, \dots, \mathbf{k}_{r+1}, \mathbf{p}_1, -\mathbf{p}_1, \dots, \mathbf{p}_n, -\mathbf{p}_n) P_L(p_1) \dots P_L(p_n). \end{aligned} \quad (36)$$

This expression means that the density fluctuation with the $(r+1)$ order of the Wiener Hermite expansion is the sum of all the $(2n+r+1)$ order of SPT.

We can understand the relation between the SPT and the Wiener Hermite expansion in a diagrammatical representation, where there is no non-dimensional coupling constant and the order of loop is determined by the order of the linear power spectrum $P_L(k)$, that is, n -loop contributions contains the terms proportional to $(P_L)^{n+1}$. Each order of the Wiener Hermite expansion includes all vertex loop contributions which come from the coefficients $\delta^{(r)}$ themselves. The order of the vertex loop is expressed by n ($n \geq 0$). On the other hand, the loop contributions from irreducible diagrams, where the loop order is expressed by r ($r \geq 0$), arise only after calculating the power spectrum in Eq. (32) and Eq. (33) (see (Bernardeau, Crocce, & Scoccimarro 2008, 2012) for details).

4.3. Relation between Γ -expansion and Wiener Hermite expansion

The relation of Eq. (31) corresponds to Eq. (17) in (Bernardeau, Crocce, & Scoccimarro 2008). That is, the Wiener Hermite expansion method coincides with the Γ -expansion approach:

$$\Gamma^{(r+1)}(z, \mathbf{k}_1, \dots, \mathbf{k}_{r+1}) = \delta_{\text{WH}}^{(r+1)}(z, \mathbf{k}_1, \dots, \mathbf{k}_{r+1}) / (\delta_L(k_1) \dots \delta_L(k_{r+1})). \quad (37)$$

For $r = 0$ in Eqs. (35) (36) and (37), we have

$$\begin{aligned} \Gamma^{(1)}(k) &= \delta_{\text{WH}}^{(1)}(z, k) / \delta_L(k) \\ &= \sum_{n=0}^{\infty} a^{2n+1} (2n+1)!! \int \frac{d^3 p_1}{(2\pi)^3} \dots \frac{d^3 p_n}{(2\pi)^3} F_{2n+1}(\mathbf{k}, \mathbf{p}_1, -\mathbf{p}_1, \dots, \mathbf{p}_n, -\mathbf{p}_n) P_L(p_1) \dots P_L(p_n). \end{aligned} \quad (38)$$

Thus, the first order of the Wiener Hermite expansion, $\delta_{\text{WH}}^{(1)}$, corresponds to the propagator in the Renormalized Perturbation Theory. Furthermore, $\delta_{r+1}^{(r+1)}$ denotes the irreducible diagrams, and this is expressed by the Γ -expansion as

$$\Gamma_{\text{tree}}^{(r+1)}(z, \mathbf{k}_1, \dots, \mathbf{k}_{r+1}) = a^{r+1} \delta_{r+1}^{(r+1)}(\mathbf{k}_1, \dots, \mathbf{k}_{r+1}) / (\delta_L(k_1) \dots \delta_L(k_{r+1})). \quad (39)$$

Note that since we focus only on the SPT, we consider only growing solutions unlike the RPT.

5. Behavior of the solutions in the high- k limit

Although the WH expansion is defined and the interpretation is physically and mathematically useful for understanding the non-linear evolution of Dark Matter, we need to truncate the expansion at some order, most probably lower order such as $r = 2$ or 3 in order to make actual calculation. Then the validity for the truncation is not guaranteed immediately. Furthermore, the computational difficulties for the power spectrum gets increased very rapidly when we increase the order of truncation. In order to resolve these difficulties, we propose in this section an approximate semi-analytic expression for the full power spectrum including all order in the WH expansion by adopting the following assumption:

- The high order solutions in the SPT become dominant in the high- k limit. Therefore, they are approximated well enough by the ones in the high- k limit.

Here, we show the exponential behavior of the solutions using the SPT, which have been proved in the RPT (Crocce & Scoccimarro 2006a,b; Bernardeau, Van de Rijt, & Vernizzi 2012).

5.1. Functions F_n and G_n in the high- k limit

We prove that the functions $F_{r+n+1}(\mathbf{k}, \mathbf{k}_1, \dots, \mathbf{k}_r, \mathbf{p}_1, \dots, \mathbf{p}_n)$ and $G_{r+n+1}(\mathbf{k}, \mathbf{k}_1, \dots, \mathbf{k}_r, \mathbf{p}_1, \dots, \mathbf{p}_n)$ takes the following expression for the high- k limit.

$$\begin{aligned} F_{r+n+1}(\mathbf{k}, \mathbf{k}_1, \dots, \mathbf{k}_r, \mathbf{p}_1, \dots, \mathbf{p}_n) &\rightarrow \frac{(r+1)!}{(r+n+1)!} F_{r+1}(\mathbf{k}, \mathbf{k}_1, \dots, \mathbf{k}_r) \gamma(\mathbf{p}_1) \dots \gamma(\mathbf{p}_n), \\ G_{r+n+1}(\mathbf{k}, \mathbf{k}_1, \dots, \mathbf{k}_r, \mathbf{p}_1, \dots, \mathbf{p}_n) &\rightarrow \frac{(r+1)!}{(r+n+1)!} G_{r+1}(\mathbf{k}, \mathbf{k}_1, \dots, \mathbf{k}_r) \gamma(\mathbf{p}_1) \dots \gamma(\mathbf{p}_n), \end{aligned} \quad (40)$$

with

$$\gamma(\mathbf{p}) \equiv \frac{\mathbf{p} \cdot \mathbf{k}}{p^2}. \quad (41)$$

Here, we define the high- k limit as

$$|\mathbf{k}| \gg \{|\mathbf{p}_i|, i = 1, 2, \dots, n\}. \quad (42)$$

From now on, we shall simplify the notations: $F_{r+n+1}(\mathbf{k}, \mathbf{k}_1, \dots, \mathbf{k}_r, \mathbf{p}_1, \dots, \mathbf{p}_n) = F_{r+n+1}(\mathbf{k}, \mathbf{k}_r, \mathbf{p}_n)$ and $G_{r+n+1}(\mathbf{k}, \mathbf{k}_1, \dots, \mathbf{k}_r, \mathbf{p}_1, \dots, \mathbf{p}_n) = G_{r+n+1}(\mathbf{k}, \mathbf{k}_r, \mathbf{p}_n)$.

We prove this by the induction in n as follows. For $n = 0$, Eq. (40) is clearly satisfied. For some n , we assume

$$\begin{aligned} F_{r+n}(\mathbf{k}, \mathbf{k}_r, \mathbf{p}_{n-1}) &\rightarrow \frac{(r+1)!}{(r+n)!} F_{r+1}(\mathbf{k}, \mathbf{k}_r) \gamma(\mathbf{p}_1) \dots \gamma(\mathbf{p}_{n-1}), \\ G_{r+n}(\mathbf{k}, \mathbf{k}_r, \mathbf{p}_{n-1}) &\rightarrow \frac{(r+1)!}{(r+n)!} G_{r+1}(\mathbf{k}, \mathbf{k}_r) \gamma(\mathbf{p}_1) \dots \gamma(\mathbf{p}_{n-1}). \end{aligned} \quad (43)$$

Then we show that $n + 1$ order satisfies the same limit.

The functions $F_{r+n+1}(\mathbf{k}, \mathbf{k}_r, \mathbf{p}_n)$ and $G_{r+n+1}(\mathbf{k}, \mathbf{k}_r, \mathbf{p}_n)$ are given by Eq. (19) and Eq. (20). Then, let us examine which terms become dominant in the high- k limit in these recursion relations. From Eq. (42), we keep only terms with the scale-dependence as $(k/p_1) \dots (k/p_n)$. Then, we have the terms proportional to $F_{r+n}(\mathbf{k}, \mathbf{k}_i, \mathbf{p}_n)$, $G_{r+n}(\mathbf{k}, \mathbf{k}_i, \mathbf{p}_n)$ for $i \leq r$, and $\gamma(\mathbf{p}_n) F_{r+n}(\mathbf{k}, \mathbf{k}_r, \mathbf{p}_{n-1})$ and $\gamma(\mathbf{p}_n) G_{r+n}(\mathbf{k}, \mathbf{k}_r, \mathbf{p}_{n-1})$ in the high- k limit. This means that the recursion relation for $F_{r+n+1}(\mathbf{k}, \mathbf{k}_r, \mathbf{p}_n)$

becomes in the high- k limit as follows.

$$\begin{aligned}
F_{r+n+1}(\mathbf{k}, \mathbf{k}_r, \mathbf{p}_n) &\rightarrow \frac{1}{(2(r+n)+5)(r+n)} \left\{ \right. \\
(2(r+n)+3) &\frac{C(r,m)}{C(n+r+1,m)} \left[\sum_{m=1}^r G_m(\mathbf{k}_m) \alpha(\mathbf{k}_{1m}, \mathbf{k} + \mathbf{k}_{(m+1)r} + \mathbf{p}_{1n}) F_{r+n+1-m}(\mathbf{k}, \mathbf{k}_{m+1}, \dots, \mathbf{k}_r, \mathbf{p}_n) \right. \\
&\quad \left. + \sum_{m=1}^r G_{r+n+1-m}(\mathbf{k}, \mathbf{k}_{m+1}, \dots, \mathbf{k}_r, \mathbf{p}_n) \alpha(\mathbf{k} + \mathbf{k}_{(m+1)r} + \mathbf{p}_{1n}, \mathbf{k}_{1m}) F_m(\mathbf{k}_m) \right] \\
&+ 4 \frac{C(r,m)}{C(n+r+1,m)} \left[\sum_{m=1}^r G_m(\mathbf{k}_m) \beta(\mathbf{k}_{1m}, \mathbf{k} + \mathbf{k}_{(m+1)r} + \mathbf{p}_{1n}) G_{r+n+1-m}(\mathbf{k}, \mathbf{k}_{m+1}, \dots, \mathbf{k}_r, \mathbf{p}_n) \right] \\
&+ (2(r+n)+3) \left(\frac{n}{r+n+1} \right) \alpha(\mathbf{p}_n, \mathbf{k} + \mathbf{k}_{1r} + \mathbf{p}_{1(n-1)}) F_{r+n}(\mathbf{k}, \mathbf{k}_r, \mathbf{p}_{n-1}) \\
&\left. + 4 \left(\frac{n}{r+n+1} \right) \beta(\mathbf{p}_n, \mathbf{k} + \mathbf{k}_{1r} + \mathbf{p}_{1(n-1)}) G_{r+n}(\mathbf{k}, \mathbf{k}_r, \mathbf{p}_{n-1}) \right\}, \tag{44}
\end{aligned}$$

where we denote as $\mathbf{k}_{(m+1)r} \equiv \mathbf{k}_{m+1} + \dots + \mathbf{k}_r$ and $\mathbf{p}_{1(n-1)} \equiv \mathbf{p}_1 + \dots + \mathbf{p}_{n-1}$, and define as

$$C(n, r) \equiv \frac{n!}{r!(n-r)!}. \tag{45}$$

Furthermore, the behavior of α and β in the high- k limit are

$$\begin{aligned}
\alpha(\mathbf{k}_{1m}, \mathbf{k} + \mathbf{k}_{(m+1)r} + \mathbf{p}_{1n}) &\rightarrow \alpha(\mathbf{k}_{1m}, \mathbf{k} + \mathbf{k}_{(m+1)r}), \\
\alpha(\mathbf{k} + \mathbf{k}_{(m+1)r} + \mathbf{p}_{1n}, \mathbf{k}_{1m}) &\rightarrow \alpha(\mathbf{k} + \mathbf{k}_{(m+1)r}, \mathbf{k}_{1m}), \\
\beta(\mathbf{k}_{1m}, \mathbf{k} + \mathbf{k}_{(m+1)r} + \mathbf{p}_{1n}) &\rightarrow \beta(\mathbf{k}_{1m}, \mathbf{k} + \mathbf{k}_{(m+1)r}), \\
\alpha(\mathbf{p}_n, \mathbf{k} + \mathbf{k}_{1r} + \mathbf{p}_{1(n-1)}) &\rightarrow \gamma(\mathbf{p}_n), \\
\beta(\mathbf{p}_n, \mathbf{k} + \mathbf{k}_{1r} + \mathbf{p}_{1(n-1)}) &\rightarrow \frac{\gamma(\mathbf{p}_n)}{2},
\end{aligned}$$

and then Eq (44) becomes

$$\begin{aligned}
F_{r+n+1}(\mathbf{k}, \mathbf{k}_r, \mathbf{p}_n) &\rightarrow \frac{1}{(2(r+n)+5)(r+n)} \left(\frac{(r+1)!}{(r+n+1)!} \right) \gamma(\mathbf{p}_1) \dots \gamma(\mathbf{p}_n) \\
&\times \left\{ (2(r+n)+3) \left[\sum_{m=1}^r G_m(\mathbf{q}_m) \alpha(\tilde{\mathbf{k}}_1, \tilde{\mathbf{k}}_2) F_{r+1-m}(\mathbf{q}_{m+1}, \dots, \mathbf{q}_{r+1}) \right] \right. \\
&\quad \left. + 2 \left[\sum_{m=1}^r G_m(\mathbf{q}_m) \beta(\tilde{\mathbf{k}}_1, \tilde{\mathbf{k}}_2) G_{r+1-m}(\mathbf{q}_{m+1}, \dots, \mathbf{q}_{r+1}) \right] \right. \\
&\quad \left. + (2(r+n)+3)n F_{r+1}(\mathbf{k}, \mathbf{k}_r) + 2n G_{r+1}(\mathbf{k}, \mathbf{k}_r) \right\}, \tag{46}
\end{aligned}$$

where $\{\mathbf{q}_1, \dots, \mathbf{q}_{r+1}\} = \{\mathbf{k}, \mathbf{k}_1, \dots, \mathbf{k}_r\}$ and $\tilde{\mathbf{k}}_1 = \mathbf{q}_{1m}$, $\tilde{\mathbf{k}}_2 \equiv \mathbf{q}_{(m+1)(r+1)}$.

From Eq. (19) and Eq. (20), we can show the following relations.

$$\left[\sum_{m=1}^r G_m(\mathbf{q}_m) \alpha(\tilde{\mathbf{k}}_1, \tilde{\mathbf{k}}_2) F_{r+1-m}(\mathbf{q}_{m+1}, \dots, \mathbf{q}_{r+1}) \right] = (r+1) F_{r+1}(\mathbf{k}, \mathbf{k}_r) - G_{r+1}(\mathbf{k}, \mathbf{k}_r) \quad (47)$$

$$\left[\sum_{m=1}^r G_m(\mathbf{q}_m) \beta(\tilde{\mathbf{k}}_1, \tilde{\mathbf{k}}_2) G_{r+1-m}(\mathbf{q}_{m+1}, \dots, \mathbf{q}_{r+1}) \right] = -\frac{1}{2} (3F_{r+1}(\mathbf{k}, \mathbf{k}_r) - (2r+3)G_{r+1}(\mathbf{k}, \mathbf{k}_r)) \quad (48)$$

Substituting Eq. (47) and Eq. (48) into Eq. (46), we can finally derive the following relation in the high- k limit,

$$F_{r+n+1}(\mathbf{k}, \mathbf{k}_r, \mathbf{p}_n) \rightarrow \frac{(r+1)!}{(r+n+1)!} \gamma(\mathbf{p}_1) \dots \gamma(\mathbf{p}_n) F_{r+1}(\mathbf{k}, \mathbf{k}_r). \quad (49)$$

Similarly, for G_{r+n+1} we can show the following relation

$$G_{r+n+1}(\mathbf{k}, \mathbf{k}_r, \mathbf{p}_n) \rightarrow \frac{(r+1)!}{(r+n+1)!} \gamma(\mathbf{p}_1) \dots \gamma(\mathbf{p}_n) G_{r+1}(\mathbf{k}, \mathbf{k}_r). \quad (50)$$

This ends the proof.

5.2. Power Spectrum in the high- k limit

We calculate the coefficients of the WH expansion in the high- k limit,

$$\begin{aligned} \delta_{\text{WH}}^{(r+1)}(z, \mathbf{k} - \mathbf{k}_{1r}, \mathbf{k}_r) &= \sum_{n=0}^{\infty} a^{2n+r+1} \delta_{2n+r+1}^{(r+1)}(\mathbf{k} - \mathbf{k}_{1r}, \mathbf{k}_r) \\ &\rightarrow \sum_{n=0}^{\infty} a^{2n+r+1} \delta_L(|\mathbf{k} - \mathbf{k}_{1r}|) \delta_L(k_1) \dots \delta_L(k_r) \\ &\quad \times F_{r+1}(\mathbf{k} - \mathbf{k}_{1r}, \mathbf{k}_r) \frac{1}{2^n n!} \left[-\frac{k^2}{6\pi^2} \int dp P_L(p) \right]^n \\ &= \exp\left(-\frac{k^2 \sigma_v^2}{2}\right) \delta_L(z, |\mathbf{k} - \mathbf{k}_{1r}|) \delta_L(z, k_1) \dots \delta_L(z, k_r) F_{r+1}(\mathbf{k} - \mathbf{k}_{1r}, \mathbf{k}_r) \\ &= \exp\left(-\frac{k^2 \sigma_v^2}{2}\right) \delta_{r+1}^{(r+1)}(z, \mathbf{k} - \mathbf{k}_{1r}, \mathbf{k}_1, \dots, \mathbf{k}_r), \end{aligned} \quad (51)$$

where we have used Eqs. (36) (40) and $(2n)!! = 2^n n!$. We define σ_v^2 as

$$\sigma_v^2 \equiv \frac{1}{6\pi^2} \int dp P_L(z, p). \quad (52)$$

Note that we define the z -dependent quantities such as $\delta_L(z, k)$ and $P_L(z, k)$ by multiplying the scale factor a , but we assume that the scale factor can be replaced by the growth factor $D(z)$ in the general cosmological models, for which $\Omega_\Lambda \neq 0$: $\delta_L(z, k) \equiv a\delta_L(k) \rightarrow D(z)\delta_L(k)$ and $P_L(z, p) \equiv a^2P_L(p) \rightarrow D^2P_L(p)$. This relation in Eq. (51) is equivalent to Eq. (42) in (Bernardeau, Crocce, & Scoccimarro 2008) from the relation between $\delta_{r+1}^{(r+1)}$ and Γ_{tree} in Eq. (39).

Then, we describe the full power spectrum in the high- k limit as

$$P(z, k) \rightarrow \exp(-k^2\sigma_v^2) \sum_{r=0}^{\infty} P_{\text{irr}}^{(r+1)}(z, k), \quad (53)$$

where

$$\begin{aligned} P_{\text{irr}}^{(r+1)}(z, k) &\equiv (r+1)! \int \frac{d^3k_1}{(2\pi)^3} \dots \int \frac{d^3k_r}{(2\pi)^3} [\delta_{r+1}^{(r+1)}(z, \mathbf{k} - \mathbf{k}_{1r}, \mathbf{k}_1, \dots, \mathbf{k}_r)]^2 \\ &= (r+1)! \int \frac{d^3k_1}{(2\pi)^3} \dots \int \frac{d^3k_r}{(2\pi)^3} [F_{r+1}(\mathbf{k} - \mathbf{k}_{1r}, \mathbf{k}_r)]^2 P_L(z, |\mathbf{k} - \mathbf{k}_{1r}|) P_L(z, k_1) \dots P_L(z, k_r). \end{aligned} \quad (54)$$

The P_{irr} includes the contributions from all the irreducible diagrams.

Here, we take further high- k limit in Eq. (54).

$$\mathbf{k} \gg \{|\mathbf{k}_i|, i = 1, \dots, r\}. \quad (55)$$

Using Eq. (40), we show

$$\begin{aligned} P_{\text{irr}}^{(r+1)} &\rightarrow (r+1)!(r+1) \int \frac{d^3k_1}{(2\pi)^3} \dots \int \frac{d^3k_r}{(2\pi)^3} [\delta_{r+1}^{(r+1)}(z, \mathbf{k}, \mathbf{k}_1, \dots, \mathbf{k}_r)]^2 \\ &\rightarrow \frac{(k^2\sigma_v^2)^r}{r!} P_L(z, k). \end{aligned} \quad (56)$$

Note the limit of $\mathbf{k} \gg \mathbf{k}_r$ ($r \geq 1$) is equal to the approximation that the most effective region of \mathbf{k}_r to their each integral is around $\mathbf{k}_r \rightarrow 0$. However, since \mathbf{k}_r have integral range of $0 \leq k_r < \infty$, there necessarily exist the case of $\mathbf{k}_r \sim \mathbf{k}$ in the integral. For $\mathbf{k}_1 \sim \mathbf{k} \gg \mathbf{k}_r$ ($\mathbf{k}_r \geq 2$), we have

$$\begin{aligned} P_{\text{irr}}^{(r+1)} &= (r+1)! \int \frac{d^3k_1}{(2\pi)^3} \dots \int \frac{d^3k_r}{(2\pi)^3} [\delta_{r+1}^{(r+1)}(z, \mathbf{k} - \mathbf{k}_{1r}, \mathbf{k}_1, \dots, \mathbf{k}_r)]^2 \\ &\rightarrow (r+1)! \int \frac{d^3q}{(2\pi)^3} \frac{d^3k_2}{(2\pi)^3} \dots \int \frac{d^3k_r}{(2\pi)^3} [\delta_{r+1}^{(r+1)}(z, \mathbf{q}, \mathbf{k}, \mathbf{k}_2, \dots, \mathbf{k}_r)]^2, \end{aligned} \quad (57)$$

where we defined \mathbf{k} as $\mathbf{k} - \mathbf{k}_{1r} \sim \mathbf{k} - \mathbf{k}_1 \equiv \mathbf{q}$. This is equal to the case of the high- k limit. The same discussion is applied for arbitrary \mathbf{k}_r . Therefore, the factor $(r+1)$ is multiplied in Eq. (56).

From Eq. (56) and Eq. (53), we finally derive

$$\begin{aligned} P(z, k) &\rightarrow P_L(z, k) \exp(-k^2\sigma_v^2) \sum_{r=0}^{\infty} \frac{(k^2\sigma_v^2)^r}{r!} \\ &= P_L(z, k). \end{aligned} \quad (58)$$

Surprisingly, the solutions in the high- k limit cancel each other, and the full power spectrum reduces to the linear power spectrum. This fact is well known in 1-loop level of the SPT (Makino, Sasaki, & Suto 1992), but it is interesting that this cancellation also applies for the dominant terms in the high- k limit in the full power spectrum. Of course, it is really not that the full power spectrum becomes the linear power spectrum in the high- k limit, because we have chosen only dominant terms in the high- k limit in the proof of Eq. (40) and Eq. (56), and the sub-leading terms can also affect to the full power spectrum even in the high- k limit. This result implies that the non-linear corrections for the power spectrum generally tend to cancel each other, and result in the small corrections as specifically known for 1 and 2-loop cases of the SPT.

5.3. Approximate Full Power Spectrum

We now propose an appropriate interpolation between the low- k and high- k solutions. The former is the 1-loop solutions in the SPT, and the later is Eq. (53) derived in the previous subsection.

In order to have an expression applicable for the case of $r = 0$, we use Eq. (40) in the following

$$F_{2n+1}(\mathbf{k}, \mathbf{p}_1, -\mathbf{p}_1, \dots, \mathbf{p}_n, -\mathbf{p}_n) \rightarrow \frac{3!}{(2n+1)!} F_3(\mathbf{k}, \mathbf{p}, -\mathbf{p}) \gamma(\mathbf{p}_2) \gamma(-\mathbf{p}_2) \dots \gamma(\mathbf{p}_n) \gamma(-\mathbf{p}_n). \quad (59)$$

Then, for $n \geq 1$, we show

$$\begin{aligned} \delta_{2n+1}^{(1)}(k) &\rightarrow \frac{2(2n+1)!!}{(2n+1)!} \left[\delta_L(k) 3 \int \frac{d^3 p_1}{(2\pi)^3} F_3(\mathbf{k}, \mathbf{p}_1, -\mathbf{p}_1) P_L(p_1) \right] \left[\int \frac{d^3 p}{(2\pi)^3} \gamma(\mathbf{p}) \gamma(-\mathbf{p}) P_L(p) \right]^{n-1} \\ &= \delta_3^{(1)}(k) \frac{2}{2^n n!} \left[-\frac{k^2}{6\pi^2} \int dp P_L(p) \right]^{n-1}, \end{aligned} \quad (60)$$

where we have denoted the 1-loop correction term in the SPT as

$$\delta_3^{(1)}(k) = 3\delta_L(k) \int \frac{d^3 p}{(2\pi)^3} F_3(\mathbf{k}, \mathbf{p}, -\mathbf{p}) P_L(p). \quad (61)$$

Then, we derive the approximate solution of $\delta_{\text{WH}}^{(1)}$ as

$$\begin{aligned} \delta_{\text{WH}}^{(1)}(z, k) &= \sum_{n=0}^{\infty} D^{2n+1} \delta_{2n+1}^{(1)}(k) \\ &\rightarrow \delta_L(z, k) + \delta_3^{(1)}(z, k) \left(\frac{2}{-k^2 \sigma_v^2} \right) \sum_{n=1}^{\infty} \frac{1}{n!} \left(-\frac{k^2 \sigma_v^2}{2} \right)^n \\ &= \delta_L(z, k) - \frac{2\delta_3^{(1)}(z, k)}{k^2 \sigma_v^2} \left[\exp \left(-\frac{k^2 \sigma_v^2}{2} \right) - 1 \right]. \end{aligned} \quad (62)$$

where we have used the general growth factor D instead of the scale factor a . The contribution to the power spectrum $P_{\text{WH}}^{(1)}$ in Eq. (33) is

$$P_{\text{WH}}^{(1)}(z, k) \rightarrow \left[\delta_L(z, k) - \frac{2\delta_3^{(1)}(z, k)}{k^2\sigma_v^2} \left(\exp\left(-\frac{k^2\sigma_v^2}{2}\right) - 1 \right) \right]^2. \quad (63)$$

For low- k , we can expand the exponential term as $e^{-k^2\sigma_v^2/2} \sim 1 - k^2\sigma_v^2/2$, and this lead the 1-loop correction,

$$\delta_{\text{WH}}^{(1)}(z, k) \rightarrow \delta_L(z, k) + \delta_3^{(1)}(z, k). \quad (64)$$

While, for the high- k limit, $\delta_{\text{WH}}^{(1)}$ becomes coincident with $\delta_L e^{-k^2\sigma_v^2/2}$ due to the good convergence of $\delta_L + 2\delta_3^{(1)}/(k^2\sigma_v^2) \rightarrow 0$.

Next, for $r \geq 1$, we use the approximation of Eq. (53). Here, we further approximate $P_{\text{irr}}^{(r+1)}$ because it is expensive to compute the terms in the case of ($r > 2$) due to their large multiple integrals. Using the following approximation from Eq. (40),

$$F_{r+1}(\mathbf{k} - \mathbf{k}_{1r}, \mathbf{k}_1, \dots, \mathbf{k}_r) \rightarrow \frac{2!}{(r+1)!} \gamma(\mathbf{k}_2) \dots \gamma(\mathbf{k}_r) F_2(\mathbf{k} - \mathbf{k}_1, \mathbf{k}_1), \quad (65)$$

we derive the approximate solution of $P_{\text{WH}}^{(r+1)}$ as,

$$\begin{aligned} P_{\text{WH}}^{(r+1)}(z, k) &\rightarrow \exp(-k^2\sigma_v^2) (r+1)! \int \frac{d^3k_1}{(2\pi)^3} \dots \frac{d^3k_r}{(2\pi)^3} \left[\delta_{r+1}^{(r+1)}(z, \mathbf{k} - \mathbf{k}_{1r}, \mathbf{k}_1, \dots, \mathbf{k}_r) \right]^2 \\ &\rightarrow \exp(-k^2\sigma_v^2) (r+1)! \frac{2!}{(r+1)!} \frac{2!}{(r+1)!} \left(\frac{r+1}{2} \right) \int \frac{d^3k_1}{(2\pi)^3} \left[\delta_2^{(2)}(z, \mathbf{k} - \mathbf{k}_1, \mathbf{k}_1) \right]^2 (k^2\sigma_v^2)^{r-1} \\ &\rightarrow \exp(-k^2\sigma_v^2) \frac{P_{22}(z, k)}{k^2\sigma_v^2} \frac{1}{r!} (k^2\sigma_v^2)^r, \end{aligned} \quad (66)$$

where we multiply the factor $(r+1)/2$ by the same reason for Eq. (56). We have denoted another 1-loop correction term in the SPT as,

$$P_{22}(z, k) = 2 \int \frac{d^3p}{(2\pi)^3} [F_2(\mathbf{k} - \mathbf{p}, \mathbf{p})]^2 P_L(z, |\mathbf{k} - \mathbf{p}|) P_L(z, p). \quad (67)$$

Indeed, when for $r = 1$ the exponential factor is expanded as $e^{-k^2\sigma_v^2} \sim 1$, the 1-loop correction, P_{22} , is reproduced in Eq. (66).

Finally, we achieve the approximate full power spectrum,

$$\begin{aligned} P(z, k) &= \sum_{r=0}^{\infty} P_{\text{WH}}^{(r+1)}(z, k) \\ &\rightarrow \left[\delta_L(z, k) - \frac{2\delta_3^{(1)}(z, k)}{k^2\sigma_v^2} \left(\exp\left(-\frac{k^2\sigma_v^2}{2}\right) - 1 \right) \right]^2 + \exp(-k^2\sigma_v^2) \frac{P_{22}(z, k)}{k^2\sigma_v^2} \sum_{r=1}^{\infty} \frac{1}{r!} (k^2\sigma_v^2)^r, \\ P_{\text{AF}}(z, k) &\equiv \left[\delta_L(z, k) - \frac{2\delta_3^{(1)}(z, k)}{k^2\sigma_v^2} \left(\exp\left(-\frac{k^2\sigma_v^2}{2}\right) - 1 \right) \right]^2 + \frac{P_{22}(z, k)}{k^2\sigma_v^2} [1 - \exp(-k^2\sigma_v^2)]. \end{aligned} \quad (68)$$

This is the main result in this paper. This give an appropriate interpolation between the low- k solutions and the high- k limit ones. We can derive the approximate solutions of each order in the Wiener Hermite expansion and the SPT using the approximation such as Eq. (59) and Eq. (65), and therefore we call this method as “Approximate Full Wiener Hermite (AFWH)” expansion method or “Approximate Full Perturbation Theory (AFPT)”. We can easily compute the solution Eq. (68) numerically, because the solution has only single or double integrals.

6. Comparison with other analytic predictions and N -body simulations

We compare the approximate full power spectrum, P_{ap} , in Eq. (68) with some other analytic predictions and N -body simulations. We mainly use N -body simulations presented in (Taruya et al. 2009), but in Sec. 6.3 we also use another N -body results with higher resolutions in (Valageas & Nishimichi 2011). It is plotted for the cosmological models with the WMAP 5yr (Komatsu et al. 2009). The cosmological parameters we used are $\Omega_m = 0.279$, $\Omega_\Lambda = 0.721$, $\Omega_b = 0.046$, $h = 0.701$, $n_s = 0.96$, $\sigma_8 = 0.817$.

The N -body simulation data with low-resolutions and high-resolutions in (Taruya et al. 2009) and (Valageas & Nishimichi 2011) were created by a public N -body code *GADGET2* (Springel 2005). Their initial conditions were generated by the *2LPT* code (Crocce, Pueblas, & Scoccimarro 2006) at $z_{\text{ini}} = 31$ and $z_{\text{ini}} = 99$, respectively. While the N -body simulations with low-resolutions were computed with cubic box sizes $1h^{-1}\text{Gpc}$, 512^3 particles, the N -body results with high-resolutions contains $2,048^3$ particles and were computed by combining the results with different box sizes, $2,048 h^{-1}\text{Mpc}$ and $4,096 h^{-1}\text{Mpc}$, called L11-N11 and L12-N11. Although the realization of the simulations with high-resolutions is only one, the simulations with low-resolutions has the output data of 30 independent realizations, and consider the correction of the finite-mode sampling by (Nishimichi et al. 2009). Therefore, the size of each error bar for N -body results with low-resolutions becomes hard to see visually. For detail of N -body simulation which is used in this paper, see Taruya et al. (Taruya et al. 2009) and Okamura et al. (Okamura, Taruya, & Matsubara 2011).

6.1. Comparison with other analytical predictions: 1-loop level

Bernardeau, Crocce, & Scoccimarro (2012) proposed a simple scheme to interpolate between the low- k and high- k solutions, based on the Γ -expansion method. In the scheme, the solutions are regularized so that the low- k solutions become the ones in the SPT and the high- k solutions become Eq. (53). We call this scheme “Regularized Γ -expansion”. From Eqs. (20) (51) in (Bernardeau, Crocce, & Scoccimarro 2012; Taruya et al. 2012), its 1-loop solution for the power

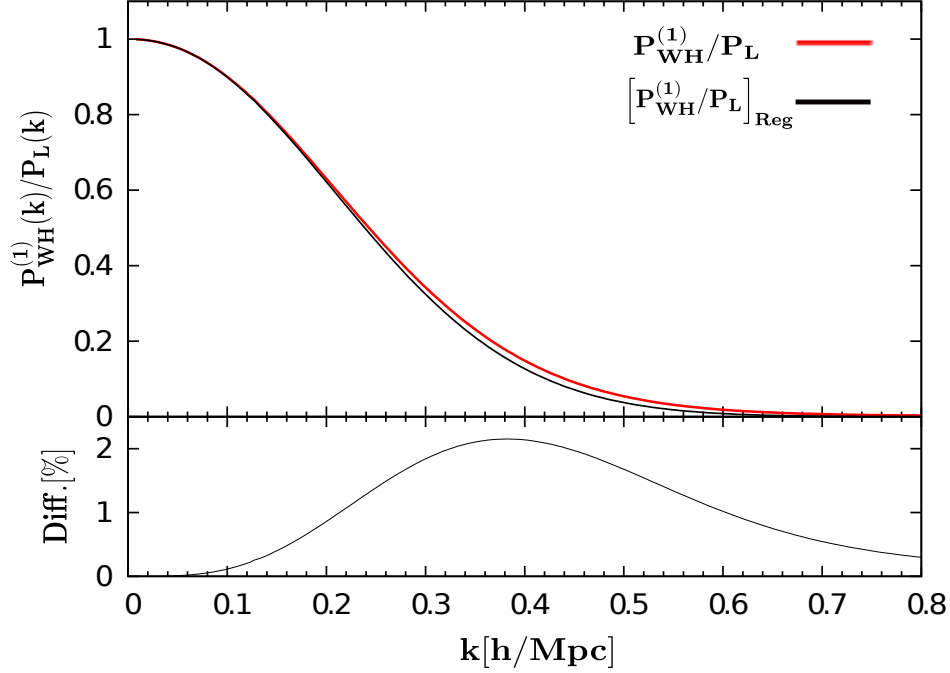


Fig. 1.— Comparison between $P_{\text{WH}}^{(1)}$ in Eq. (63) (red line) and $[P_{\text{WH}}^{(1)}]_{\text{Reg}}$ in Eq. (70) (black line) for $P_{\text{WH}}^{(1)}/P_L$ at $z = 1$. The fractional difference, $(P_{\text{WH}}^{(1)} - [P_{\text{WH}}^{(1)}]_{\text{Reg}})/P_L$, is also plotted.

spectrum is given by

$$P_{\text{Reg}} = \exp(-k^2\sigma_v^2) \left[\left(\delta_L + \delta_3 + \frac{k^2\sigma_v^2}{2}\delta_L \right)^2 + P_{22} \right]. \quad (69)$$

Since the Wiener Hermite expansion and the Γ -expansion are completely equivalent with each other, we can understand this solution as the truncation up to the second order in the Wiener Hermite expansion, and write $P_{\text{WH}}^{(1)}$ using the Regularized Γ -expansion as

$$\left[P_{\text{WH}}^{(1)} \right]_{\text{Reg}} = \exp(-k^2\sigma_v^2) \left[\delta_L + \delta_3 + \frac{k^2\sigma_v^2}{2}\delta_L \right]^2. \quad (70)$$

The difference between Eq. (63) and Eq. (70) is the way of the interpolation for the solutions. While the Regularized Γ -expansion method is a heuristic scheme, we have used the approximation of Eq. (59).

When we ignore the contributions of $P_{\text{WH}}^{(r+1)}$ ($r > 2$), we derive the solution of the approximate Wiener Hermite expansion corresponding the Regularized Γ -expansion in Eq. (69) as

$$P_{\text{WH}}^{(1)} + P_{\text{WH}}^{(2)} = \left[\delta_L(z, k) - \frac{2\delta_3^{(1)}(z, k)}{k^2\sigma_v^2} \left(\exp\left(-\frac{k^2\sigma_v^2}{2}\right) - 1 \right) \right]^2 + \exp(-k^2\sigma_v^2)P_{22}(z, k). \quad (71)$$

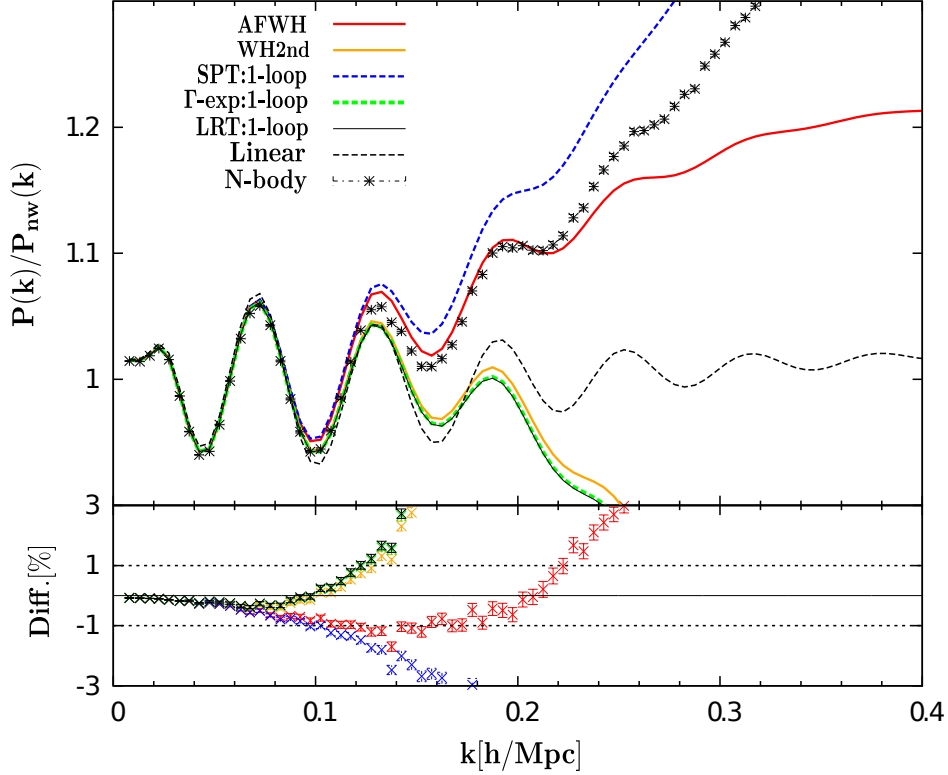


Fig. 2.— Comparison between N -body results and some analytical predictions in the case of WMAP 5 year cosmological parameters. The results at redshifts $z = 1$ up to $k = 0.4 \text{ hMpc}^{-1}$ are shown. We show the ratio of the predicted power spectra to the smoothed reference spectra, $P(k)/P_{\text{nw}}(k)$, (Blue dashed, green dashed, black solid, orange solid, red solid lines, and black symbols are, respectively, 1-loop SPT, Regularized Γ -expansion, LRT, 2nd order of WH expansion in Eq. (71) and AFWH in Eq. (68) predictions and N -body simulation result.), and the fractional difference between N -body and analytic predicted results, $[P_{\text{Nbody}}(k) - P(k)]/P_{\text{nw}}(k)$, (Blue, green, orange, black and red symbols are the fractional difference between N -body and 1-loop, Regularized Γ -expansion, 2nd order of WH expansion, LRT, and AFWH.).

We plot these two solutions, $P_{\text{WH}}^{(1)}/P_L$ and $[P_{\text{WH}}^{(1)}]_{\text{Reg}}/P_L$, and their fractional difference, $(P_{\text{WH}}^{(1)} - [P_{\text{WH}}^{(1)}]_{\text{Reg}})/P_L$, at $z = 1$ in Fig. 1. On BAO scales ($\sim 0.2 \text{ hMpc}^{-1}$), the fractional difference is within 1 %. On high- k , our solution becomes slightly larger than the Regularized Γ -expansion. However, there is no meaning in investigating which results are more accuracy in detail, because on such scales the amplitude of $P_{\text{WH}}^{(1)}$ decay due to the exponential factor enough not to largely contribute to the full power spectrum.

In Fig. 2, we plot the various analytic solutions with 1-loop level corrections and N -body simulation result (blue dashed: SPT, green dashed: Regularized Γ -expansion, black solid: LRT,

orange solid: $P_{\text{WH}}^{(1)} + P_{\text{WH}}^{(2)}$ in Eq. (71), red solid: AFWH in Eq. (68), and N -body result: black symbols) at $z = 1$.¹ To easily see the BAO, we plot the ratio of power spectrum to a smooth reference spectrum, $P(k)/P_{\text{nw}}(k)$, where the function $P_{\text{nw}}(k)$ is the linear power spectrum calculated from the smoothed transfer function neglecting the BAO feature in (Eisenstein & Hu 1998). To investigate the agreement with N -body results in more quantitative ways, we also plot the fractional differences between N -body simulations and the predicted power spectrum $P(k)$, i.e., $[P_{\text{Nbody}}(k) - P(k)]/P(k)$, (N -body results vs. 1-loop SPT : blue, Regularized Γ -expansion : green, LRT : black, $P_{\text{WH}}^{(1)} + P_{\text{WH}}^{(2)}$: orange, AFWH in Eq. (68) : red).

The Regularized Γ -expansion, LRT, and $P_{\text{WH}}^{(1)} + P_{\text{WH}}^{(2)}$ are very similar so that we can hardly see their difference. Their solutions improve the overestimation of the SPT, but decay at low- k soon because of their exponential factor. On the other hand, we can find that the main difference of our result from the previous works with 1-loop level is the higher order of the Wiener Hermite expansion, $P_{\text{WH}}^{(r+1)}$ ($r \geq 2$). Because of these terms, the AFWH in Eq. (68) (red solid line) does not decay and keep the values well around N -body simulations on BAO scales.

6.2. Comparison with 2-loop solutions in the SPT

A merit of our interpolation is that we can directly compare our approximate solutions with ones of each order in the perturbation theory. In previous works, the validity of the predicted power spectra have been verified only by comparing with the N -body results. However, we can verify the validity of our approximation such as Eq. (62) and Eq. (66) by comparing with the 2-loop solutions in the SPT. The 2-loop corrections are give by

$$P_{2\text{loop}} = P_{15} + P_{24} + P_{33} + \left[\delta_3^{(1)} \right]^2, \quad (74)$$

where each term is calculated, respectively, as

$$\begin{aligned} P_{15}(z, k) &= 30P_L(z, k) \int \frac{d^3p_1}{(2\pi)^3} \frac{d^3p_2}{(2\pi)^3} F_5(\mathbf{k}, \mathbf{p}_1, -\mathbf{p}_1, \mathbf{p}_2, -\mathbf{p}_2) P_L(z, p_1) P_L(z, p_2), \\ P_{24}(z, k) &= 24 \int \frac{d^3p_1}{(2\pi)^3} \frac{d^3p_2}{(2\pi)^3} F_2(\mathbf{k} - \mathbf{p}_1, \mathbf{p}_1) F_4(\mathbf{k} - \mathbf{p}_1, \mathbf{p}_1, \mathbf{p}_2, -\mathbf{p}_2) P_L(z, |\mathbf{k} - \mathbf{p}_1|) P_L(z, p_1) P_L(z, p_2), \\ P_{33}(z, k) &= 6 \int \frac{d^3p_1}{(2\pi)^3} \frac{d^3p_2}{(2\pi)^3} [F_3(\mathbf{k} - \mathbf{p}_1 - \mathbf{p}_2, \mathbf{p}_1, \mathbf{p}_2)]^2 P_L(z, |\mathbf{k} - \mathbf{p}_1 - \mathbf{p}_2|) P_L(z, p_1) P_L(z, p_2). \end{aligned} \quad (75)$$

¹The power spectrum of the Standard PT and LRT (Matsubara 2008b) are given by

$$P_{1\text{loop}} = P_L + P_{13} + P_{22}, \quad (72)$$

$$P_{\text{Lag}} = \exp(-k^2\sigma_v^2) (P_L + P_{13} + P_{22} + k^2\sigma_v^2 P_L), \quad (73)$$

where we denote as $P_{13} = 2\delta_L\delta_3^{(1)}$. Although the LRT is very similar to the Regularized Γ -expansion and our result, the complete correspondence for them (e.g., the origin of the exponential factor) is not trivial.

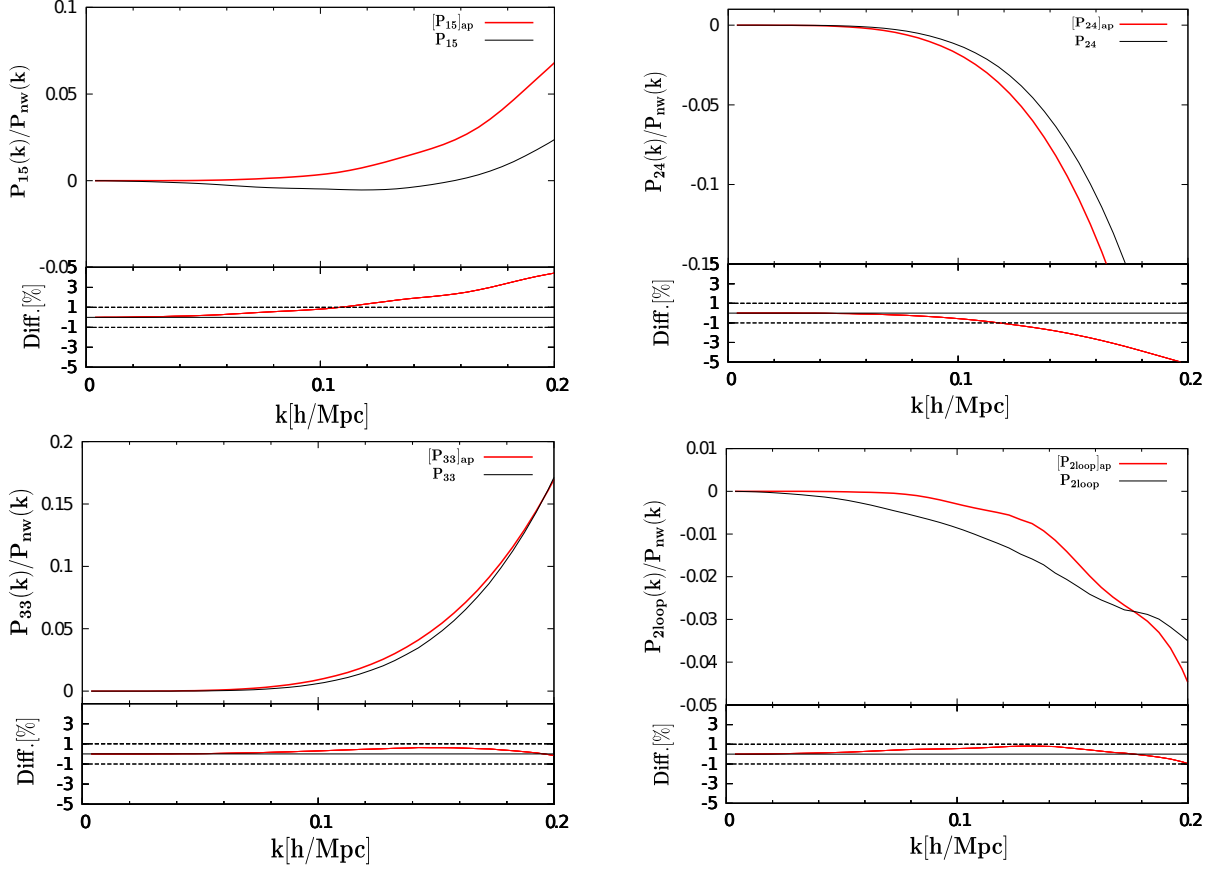


Fig. 3.— Comparison between the approximate solutions and precise ones in the SPT 2-loop level in the case of WMAP 5 year cosmological parameters at $z = 1$. We show the ratio of the power spectra to the smoothed reference spectra, P/P_{nw} , $[P]_{\text{ap}}/P_{\text{nw}}$, and the fractional difference, $[P_{\text{ap}} - P]/P_{\text{nw}}$ (top left: $P = P_{15}$, top right: P_{24} , bottom left: P_{33} , bottom right: $P_{2\text{loop}}$).

On the other hand, we show the corresponding approximate solutions using Eq. (59) and Eq. (65) as follows,

$$\begin{aligned}
 P_{15} &\rightarrow [P_{15}]_{\text{ap}} = \frac{1}{2} \left(-\frac{k^2 \sigma_v^2}{2} \right) P_{13}, \\
 P_{24} &\rightarrow [P_{24}]_{\text{ap}} = -(k^2 \sigma_v^2) P_{22}, \\
 P_{33} &\rightarrow [P_{33}]_{\text{ap}} = \left(\frac{k^2 \sigma_v^2}{2} \right) P_{22},
 \end{aligned} \tag{76}$$

$$P_{2\text{loop}} \rightarrow [P_{2\text{loop}}]_{\text{ap}} = -\frac{k^2 \sigma_v^2}{4} P_{13} - \frac{k^2 \sigma_v^2}{2} P_{22} + [\delta_3^{(1)}]^2. \tag{77}$$

Here, we have not considered the approximation of the term $[\delta_3^{(1)}]^2$, because it is the square of the 1loop term and we can easily compute it.

In Fig. 3, we plot the correct 2-loop solutions, their approximate solutions, and their fractional difference, $[(P]_{\text{ap}} - P]/P_{\text{nw}}$, ($P = P_{15}, P_{24}, P_{33}$, and $P_{2\text{loop}}$), in each panel. We plot the solutions up to $0.2h\text{Mpc}^{-1}$ at $z = 1$, because the 2-loop corrections give the good result about up to the scales (see (Okamura, Taruya, & Matsubara 2011)).

For P_{15} and P_{24} in top panels, the approximate solutions respectively overestimate and underestimate about 5 % at $k = 0.2h\text{Mpc}^{-1}$. On the other hand, for P_{33} in bottom left panel, the approximate solution gives the very good coincidence with the precise solution within 1 %. One may think that since there are large difference for P_{15} and P_{24} , our approximation is not valid. However, remember that each correction term in the perturbation theory tend to cancel and result in small corrections. Therefore, if the approximate solution for P_{15} overestimate, it is natural that there is the underestimation for other solutions such as P_{24} to cancel the overestimated solutions. As a result, for full 2-loop corrections in the bottom right panel, the fractional difference becomes within 1 % up to $0.2h\text{Mpc}^{-1}$.

6.3. Comparison with closure theory

Finally, we compare with the closure theory (2nd Born) in (Taruya et al. 2009), which is the one of the best prediction at the moment. In addition, we plot high-resolution N -body simulations presented by (Valageas & Nishimichi 2011).

In Fig. 4, We plot the power spectra from Closure theory (purple dashed), AFWH in Eq. (68) (red solid), and N -body results with error bars (low-resolution: black symbols, and high-resolution: green symbols) at some redshifts ($z = 3.0, 2.0, 1.0, 0.5$). The plotted range of scales is $k \leq 0.4h\text{Mpc}^{-1}$. We also plot the fractional differences (N -body result with low-resolution vs. Closure: purple, AFWH: red, and N -body result with high-resolution vs. AFWH: green)

Overall, the predictions of the AFWH tend to overestimate the N -body simulations at low- k (BAO scales) slightly, and then begin to underestimate at high- k . The overestimation is due to the fact that we computed only 1-loop level in the SPT precisely. In fact, our approximate solutions are slightly larger than the 2-loop SPT solutions as shown Fig. 3. Therefore, to derive more precise prediction on BAO scales, we need to calculate up to the 2-loop level corrections. The reason of the underestimation is that the expression of the high- k limit would not apply perfectly in the range of calculation or the sub-leading contributions on small scales would become effective. We would need to compute the higher order of the WH expansion without the approximation to derive the precise non-linearity in the high- k range. Although our results certainly gives slightly less accuracy than the closure theory' ones, the difference is controlled within 1 % on BAO scales.

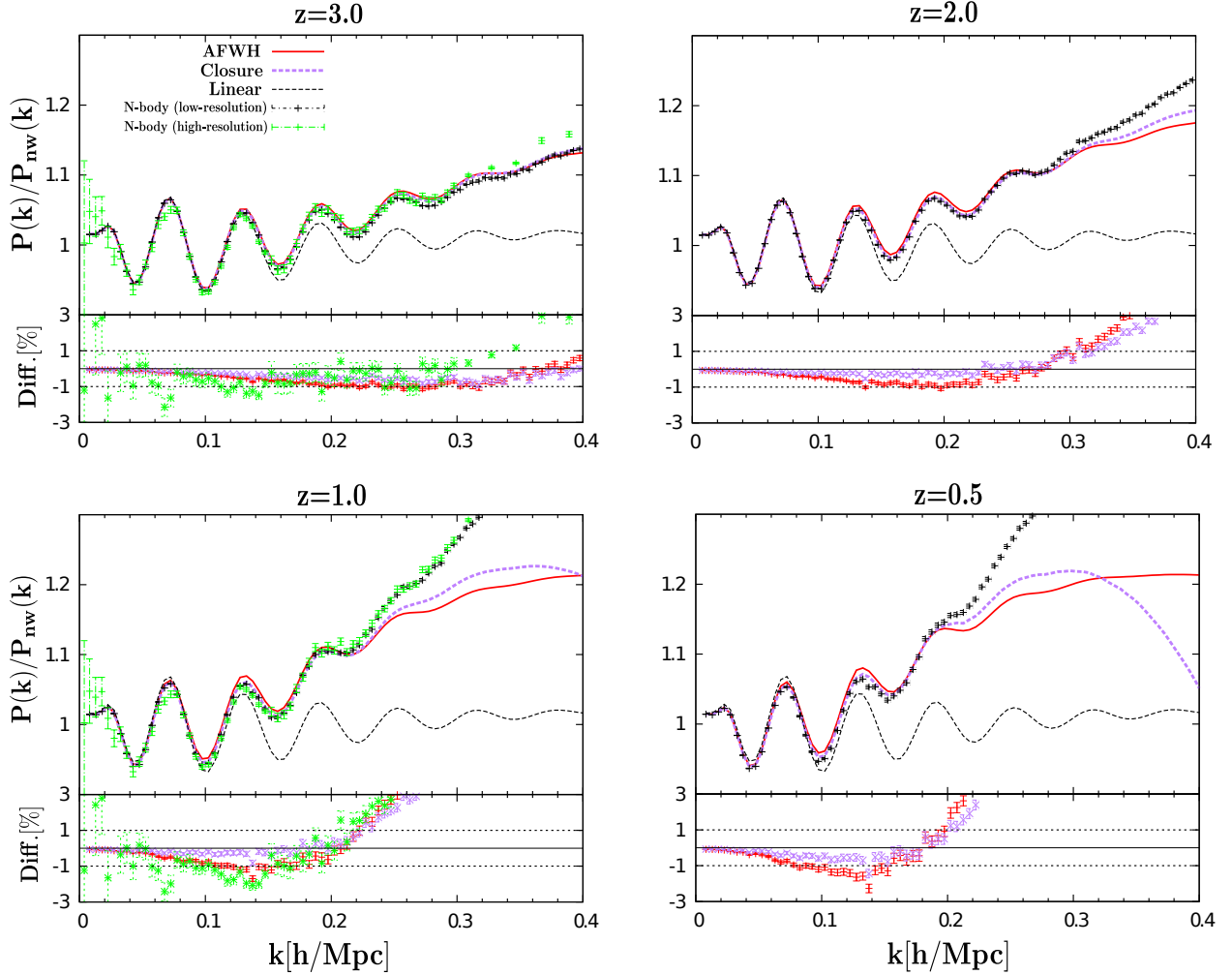


Fig. 4.— This figure is the same as in Fig. 2, but here we compare the predictions of the AFWH (red solid) with those of the closure theory (purple dashed) and N -body simulation results (green: high-resolution, black: low-resolution) at some redshifts ($z = 0.5, 1, 2, 3$). We also the fractional difference between the predicted power spectra and N -body results. The red, green and purple symbols are respectively N -body (low-resolution) vs. AFWH, N -body (high-resolution) vs. AFWH, and N -body (low-resolution) vs. closure theory.

7. Correlation function

We compute the two-point correlation function calculated from the power spectrum in Eq. (68), which is given by

$$\xi(z, r) = \int_0^\infty \frac{k^2 dk}{2\pi^2} \frac{\sin(kr)}{kr} P_{AF}(z, k). \quad (78)$$

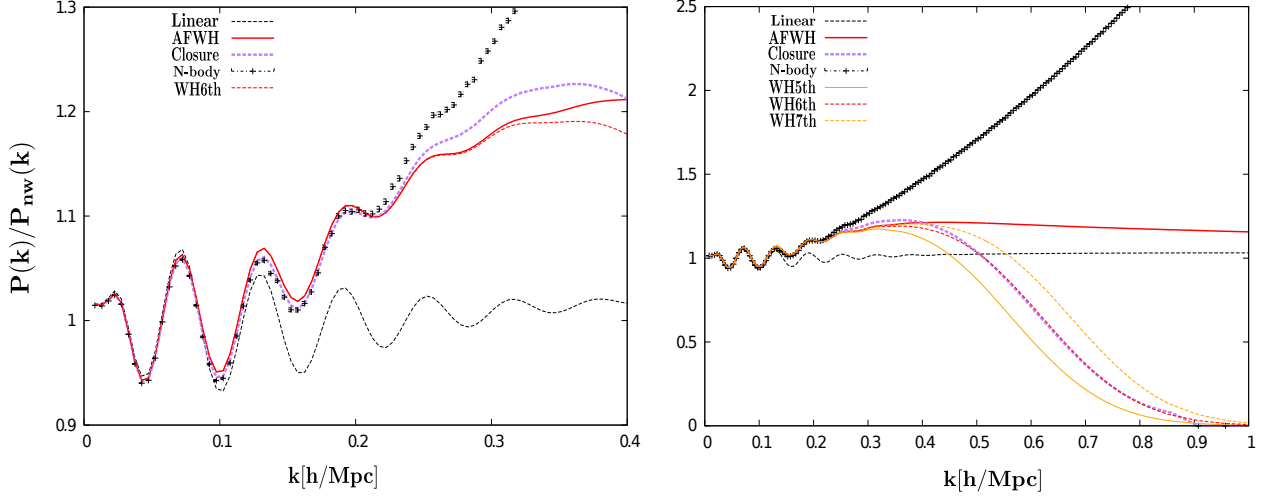


Fig. 5.— The left and right panels are the same as the bottom left panel in Fig. 4. We compare the finite truncation of the WH expansion in Eq. (81) (red dashed) with the AFWH in Eq. (68) (red line) at $z = 1$. In the right panel, we further plot the 5th, 6th and 7th order of the WH expansion up to $k = 1[h/\text{Mpc}]$.

Usually, we are not able to compute the correlation function in the SPT, because the integrand function diverge. For example, in the 1-loop level of the SPT, the predicted solution has the scale-dependence of $k^2 P_L(k)$ at high- k , because the approximate solutions of P_{13} and P_{22} are proportional to $k^2 P_L(k)$. Therefore, the integrand in Eq. (78) has the scale-dependence of $\sin(kr) \ln^2(k)$:

$$\frac{k^2}{2\pi^2} \frac{\sin(kr)}{kr} P_{1\text{loop}}(z, k) \propto \frac{k^2}{2\pi^2} \frac{\sin(kr)}{kr} k^2 P_L(k) \propto \sin(kr) \ln^2(k), \quad (79)$$

where we have used the behavior of the linear power spectrum at high- k , $P_L(k) \rightarrow \ln^2(k)/k^3$. This solution diverge in the high- k , and we are not able to evaluate the integration with the range of $0 \leq k \leq \infty$.

On the other hand, we are able to compute the correlation function for the AFWH because the solution have the scale-dependence like the linear power spectrum at high- k :

$$P_{\text{AF}}(z, k) \rightarrow \left[\delta_L(z, k) + \frac{2\delta_3^{(1)}(z, k)}{k^2 \sigma_v^2} \right]^2 + \frac{P_{22}(z, k)}{k^2 \sigma_v^2}, \quad (80)$$

$$\propto P_L(z, k).$$

In the first line, we dropped the terms including exponential factor. The scale-dependence of $\delta_3^{(1)}$ and P_{22} at high- k are proportional to $k^2 \delta_L(k)$ and $k^2 P_L(k)$. As a result, P_{AF} (red line in the right panel of Fig. 5) is proportional to P_L (black dashed in Fig. 5), and the integrand of Eq. (78) converge like the linear power spectrum.

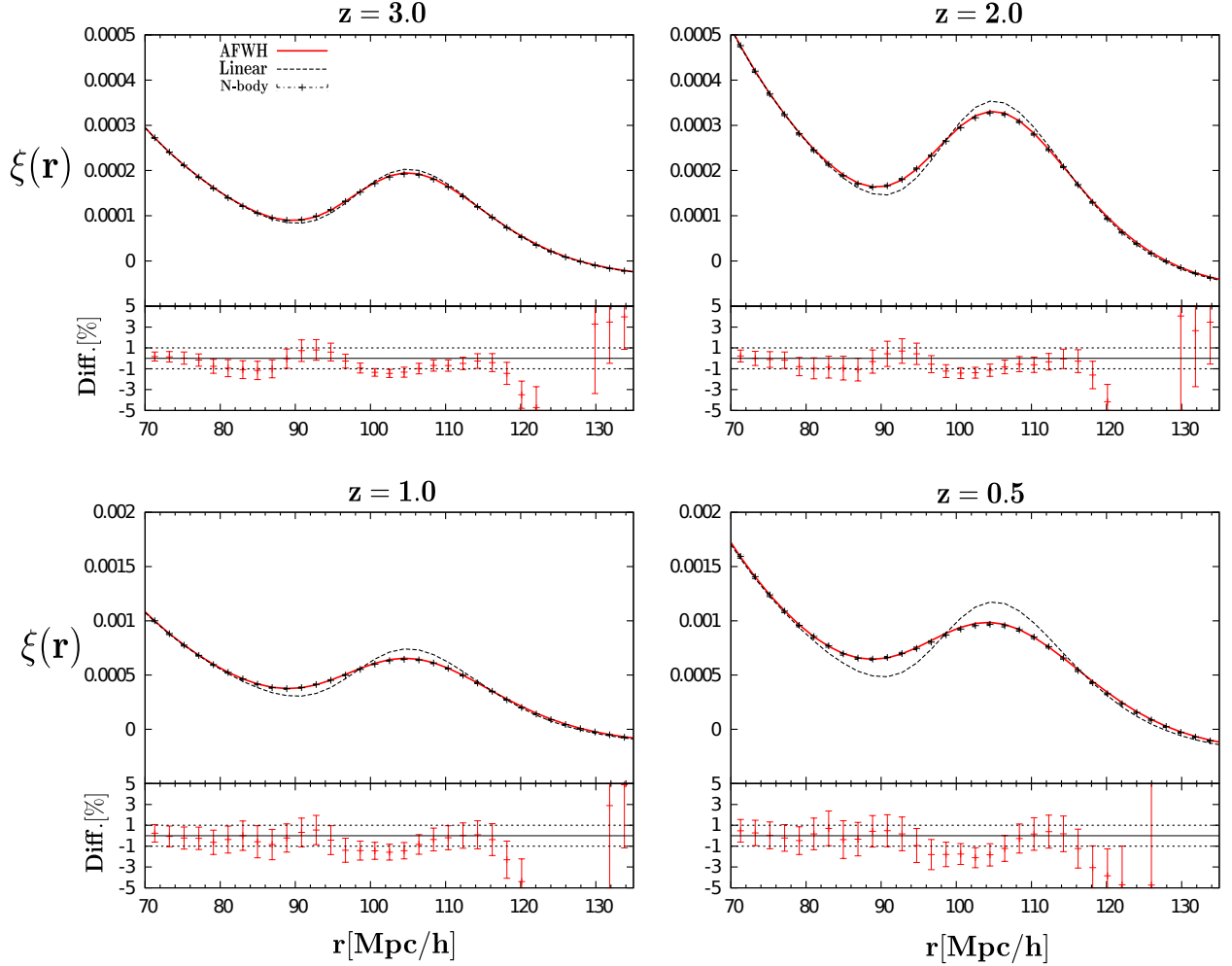


Fig. 6.— Comparison between the predicted correlation functions and N -body results (red line: AFWH, black dashed: linear theory, and black symbols: N -body simulations). The results at some redshifts ($z=0.5, 1.0, 2.0, 3.0$) with the range of $70 \leq r[\text{Mpc}/h] \leq 135$ are shown. We further plot the fractional difference between the predictions of the AFWH and N -body results, $[\xi_{\text{Nbody}}(r) - \xi(r)]/\xi(r)$.

Furthermore, as long as we focus on the BAO scales in real space ($60 \lesssim r \lesssim 140[\text{Mpc}/h]$), the behavior of the power spectrum on the small scales in Fourier space ($k \geq 0.2-0.4[h/\text{Mpc}]$) contributes very little to the result of the correlation function. Therefore, we may truncate the WH expansion up to the appropriate order so that the integrand function converge to zero due to the

exponential factor and we can easier compute the correlation function:

$$P_{\text{AF}}(z, k) \rightarrow \left[\delta_L(z, k) - \frac{2\delta_3^{(1)}(z, k)}{k^2\sigma_v^2} \left(\exp\left(-\frac{k^2\sigma_v^2}{2}\right) - 1 \right) \right]^2 + \exp(-k^2\sigma_v^2)P_{22} \left(1 + \frac{1}{2}(k^2\sigma_v^2) + \frac{1}{3!}(k^2\sigma_v^2)^2 + \frac{1}{4!}(k^2\sigma_v^2)^3 + \frac{1}{5!}(k^2\sigma_v^2)^4 \right), \quad (81)$$

where we have truncated the WH expansion up to the 6th order. We plot the solution of Eq. (81) in Fig. 5 at $z = 1$, where the difference between the AFWH in Eq. (68) (red line) and the solution of Eq. (81) (red dashed) up to $k \lesssim 0.25[h/\text{Mpc}]$ is not visible, and the solution behaves like the ones of closure theory at high- k . In the right panel of Fig. 5, we further plot the solutions of the 5th (orange line) and 7th (orange dashed) order in the WH expansion.

Here, we adopt the 6th order solution of the WH expansion to compute the correlation function in Eq. (78). In Fig. 6, we plot the analytic predictions of the correlation function, $\xi(r)$ (red line: AFWH, black dashed: linear theory, and black symbols: N -body results), and the fractional difference between the predicted correlation functions from the AFWH and the N -body simulation results, $[\xi_{\text{Nbody}}(r) - \xi(r)]/\xi(r)$.

Our predictions explain the displacement of the location of the BAO peaks and smoothing of their amplitudes due to the non-linear effects. As a result, the fractional difference against the N -body results are within 1-3 %. The almost same results are derived even for the 2nd order of the WH expansion in Eq. (71), because the contributions on small scales contribute very little to the correlation function around the BAO peak. Thus fact have been well known also in other modified PT (e.g., (Taruya et al. 2009; Okamura, Taruya, & Matsubara 2011)).

8. Conclusion

We have applied the WH expansion to the evolution equation of Dark Matter in the Newtonian gravity. It diagrammatically corresponds to the classification of the power spectrum in which each order includes all of the vertex loop contributions. It is proved that the WH expansion is mathematically equivalent with the Γ -expansion approach in the Multi-Point Propagators method.

Even if WH expansion method is physically and mathematically useful for understanding the non-linearity of evolution for Dark Matter, the validity of the finite truncation of the expansion is not clear and the difficulty of the calculation will remain. To resolve these difficulties, we proposed a way to include all order effect by assuming that the high non-linear solutions are well approximated by the ones in the high- k limit. Namely we calculate only low order terms precisely and replace the high order solutions into the ones in the high- k limit.

It have been known in the RPT that the matter density and velocity fluctuations of Dark Matter have the exponential behavior in the high- k limit. We reprovod this behavior in the context of the SPT using the WH expansion by proving that the kernel functions F and G take the forms

as Eq. (40) in the high- k limit. Using the approximate kernel functions F and G , we proposed an appropriate interpolation between high- k and low- k solutions, and the approximate full power spectrum in Eq. (68), which include the full order of the SPT approximately.

We compared our results with some other analytic predictions (e.g., Regularized Γ -expansion, LRT, SPT, closure theory) and N -body simulation results. Since the WH expansion is equivalent to the Γ -expansion and the Regularized Γ -expansion bases on the Γ -expansion, we can describe the first order of the WH expansion, $P_{\text{WH}}^{(1)}$, using the Regularized Γ -expansion in Eq. (70). One of the difference between our result and the Regularized Γ -expansion is the way of interpolation between the high- k and low- k solutions, but this difference slightly affect the predicted power spectrum. Another difference is that we consider the higher order of the WH expansion approximately. As a result, even for 1-loop level, the predicted power spectrum in Eq. (68) does not decay due to the exponential factor as shown in Fig. 2, and results in the good agreement with N -body simulation on the BAO scales.

The validity of the various modified PT (e.g., LRT, RPT, closure theory, ...) predictions is usually verified only by comparing with the N -body simulations. However, we can verify our approximation also by comparing with the solutions with the SPT 2loop level. In Fig.3, we showed that the fractional difference between the approximate solutions and the precise solutions with the SPT 2-loop level is within 1 % on BAO scales ($\leq 0.2h\text{Mpc}^{-1}$) for cosmological parameters of the WMAP 5yr at $z = 1$.

We also compared with the closure theory which is one of the best prediction at a moment, and the accuracy of the AFWH in Eq. (68) is comparable to or slightly less than the ones in the closure theory, which the fractional difference is within 1 % on BAO scales.

Finally, we computed the two-point correlation function for the AFWH. We can compute the correlation functions because the predicted power spectrum in the AFWH converge like the linear theory. Since the contributions on small scales do not affect the values of the correlation function, one may use Eq. (81) to compute the correlation function. This solution has the same behavior with Eq. (68) on BAO scales and decay on small scales due to the exponential factor in Fig. 5. The predicted correlation functions from the AFWH agree very well with the N -body simulation results, and the fractional difference are within 1 – 3 %.

We could use and apply our results to various studies for the non-linear evolution of Dark Matter (e.g., redshift distortion effect, bias effect, and bispectrum, etc.), because our prescription is easy and gives the good results comparable to the closure theory, and furthermore the computational time is very rapid.

Acknowledgments

We would like to thank T. Nishimichi and A. Taruya for providing us the numerical simulation results and useful comments and Y. Itoh, T. Okamura for useful discussion. This work is supported in part by the GCOE Program “Weaving Science Web beyond Particle-matter Hierarchy” at Tohoku University and by a Grant-in-Aid for Scientific Research from JSPS (No. 24-3849 for NSS and Nos. 18072001, 20540245 for TF) as well as by Core-to-Core Program “International Research Network for Dark Energy.” TF thanks to Luc Branchet and Institute of Astronomical Observatory, Paris for warm hospitality during his stay in the last stage of the present work.

REFERENCES

- Eisenstein, Daniel J. and Hu, Wayne and Tegmark, Max, 1998, *ApJ*, 504, L57
- Matsubara, Takahiko, 2004, *ApJ*, 615, 573
- Eisenstein, Daniel J. and others, 2005, *ApJ*, 633, 560
- Seo, Hee-Jong and Eisenstein, Daniel J., 2003, *ApJ*, 598, 720
- Blake, Chris and Glazebrook, Karl, 2003, *ApJ*, 594, 665
- Glazebrook, Karl and Blake, Chris, 2005, *ApJ*, 631, 1
- Shoji, Masatoshi and Jeong, Donghui and Komatsu, Eiichiro, 2009, *ApJ*, 693, 1404
- Padmanabhan, Nikhil and White, Martin J., 2008, *Phys. Rev. D*, 77, 123540
- Bernardeau, F. and Colombi, S. and Gaztanaga, E. and Scoccimarro, R., 2002, *Phys. Rep.*, 367, 1
- Meiksin, A. and White, Martin J. and Peacock, J. A., 1999, *MNRAS*, 304, 851
- Fry, James N., 1984, *ApJ*, 279, 499
- Goroff, M. H. and Grinstein, Benjamin and Rey, S. J. and Wise, Mark B., 1986, *ApJ*, 311, 6
- Suto, Yasushi and Sasaki, Misao, 1991, *Phys. Rev. Lett.*, 66, 264
- Makino, Nobuyoshi and Sasaki, Misao and Suto, Yasushi, 1992, *Phys. Rev. D*, 46, 585
- Jain, Bhuvnesh and Bertschinger, Edmund, 1994, *ApJ*, 431, 495
- Scoccimarro, Roman and Frieman, Josh, 1996, *ApJ*, 473, 620
- Bernardeau, F. and Colombi, S. and Gaztanaga, E. and Scoccimarro, R., 2002, *Phys. Rep.*, 367, 1
- Jeong, Donghui and Komatsu, Eiichiro, 2006, *ApJ*, 651, 619

- Jeong, Donghui and Komatsu, Eiichiro, 2009, *ApJ*, 691, 569
- Crocce, Martin and Scoccimarro, Roman, 2006, *Phys. Rev. D*, 73, 063519
- Crocce, Martin and Scoccimarro, Roman, 2006, *Phys. Rev. D*, 73, 063520
- Crocce, Martin and Scoccimarro, Roman, 2008, *Phys. Rev. D*, 77, 023533
- McDonald, Patrick, 2007, *Phys. Rev. D*, 75, 043514
- Valageas, P., 2004, *A&A*, 421, 23
- Matarrese, Sabino and Pietroni, Massimo, 2007, *J. Cosmology Astropart. Phys.*, 0706, 026
- Taruya, Atsushi and Nishimichi, Takahiro and Saito, Shun and Hiramatsu, Takashi, 2009, *Phys. Rev. D*, 80, 123503
- Hiramatsu, Takashi and Taruya, Atsushi, 2009, *Phys. Rev. D*, 79, 103526
- Pietroni, Massimo, 2008, *J. Cosmology Astropart. Phys.*, 0810, 036
- Okamura, Tomohiro and Taruya, Atsushi and Matsubara, Takahiko, 2011, *J. Cosmology Astropart. Phys.*, 1108, 012
- Bernardeau, Francis and Crocce, Martin and Scoccimarro, Roman, 2008, *Phys. Rev. D*, 78, 103521
- Bernardeau, Francis and Crocce, Martin and Sefusatti, Emiliano, 2010, *Phys. Rev. D*, 82, 083507
- Bernardeau, Francis and Van de Rijt, Nicolas and Vernizzi, Filippo, 2012, *Phys. Rev. D*, 85, 063509
- Bernardeau, Francis and Crocce, Martin and Scoccimarro, Roman, 2012, *Phys. Rev. D*, 85, 123519
- Carlson, Jordan and White, Martin and Padmanabhan, Nikhil, 2009, *Phys. Rev. D*, 80, 043531
- Scoccimarro, Roman, 1998, *MNRAS*, 299, 1097
- Matsubara, Takahiko, 2011, *Phys. Rev. D*, 83, 083518
- Matsubara, Takahiko, 2008, *Phys. Rev. D*, 78, 083519
- Matsubara, Takahiko, 2008, *Phys. Rev. D*, 77, 063530
- Valageas, Patrick and Nishimichi, Takahiro, 2011, *A&A*, 532, A4
- Komatsu, E. and others, 2009, *ApJS*, 180, 330
- Springel, Volker, 2005, *MNRAS*, 364, 1105
- Crocce, M. and Pueblas, S. and Scoccimarro, R., 2006, *MNRAS*, 373, 361

Nishimichi, Takahiro and others, 2009, PASJ, 61, 321

Eisenstein, Daniel J. and Hu, Wayne, 1998, ApJ, 496, 605

Taruya, Atsushi and Bernardeau, Francis and Nishimichi, Takahiro and Codis, Sandrine, 2012,
arXiv: 1208.1191